IJMMM International Journal of Minerals, Metallurgy and Materials 矿物冶金与材料学报（英文版）

Review on the phosphate-based conversion coatings of magnesium and its alloys

Debasis Saran, Atul Kumar, Sivaiah Bathula, David Klaumünzer, and Kisor K Sahu

Cite this article as:
Debasis Saran, Atul Kumar, Sivaiah Bathula, David Klaumünzer, and Kisor K Sahu, Review on the phosphate-based conversion coatings of magnesium and its alloys, *Int. J. Miner. Metall. Mater.*, 29(2022), No. 7, pp. 1435-1452. https://doi.org/10.1007/s12613-022-2419-2

International Journal of Minerals, Metallurgy and Materials
Volume 29, Number 7, July 2022, Page 1435
https://doi.org/10.1007/s12613-022-2419-2

Invited Review

Review on the phosphate-based conversion coatings of magnesium and its alloys

Debasis Saran[1)], *Atul Kumar*[1)], *Sivaiah Bathula*[1)], *David Klaumünzer*[2)], *and Kisor K Sahu*[1,3),✉]

1) School of Minerals, Metallurgical and Materials Engineering, Indian Institute of Technology Bhubaneswar, Bhubaneswar 752050, India
2) Group Innovation (COI Battery-Metals), Volkswagen AG, Wolfsburg 38440, Germany
3) Virtual and Augmented Reality Centre of Excellence (VARCOE), Indian Institute of Technology Bhubaneswar, Bhubaneswar 752050, India
(Received: 31 October 2021; revised: 12 January 2022; accepted: 17 January 2022)

Abstract: Magnesium (Mg) and its alloys are lightweight as well as biocompatible and possess a high strength-to-weight ratio, making them suitable for many industries, including aerospace, automobile, and medical. The major challenge is their high susceptibility to corrosion, thereby limiting their usability. The considerably lower reduction potential of Mg compared to other metals makes it vulnerable to galvanic coupling. The oxide layer on Mg offers little corrosion resistance because of its high porosity, inhomogeneity, and fragility. Chemical conversion coatings (CCs) belong to a distinct class because of underlying chemical reactions, which are fundamentally different from other types of coating. Typically, a CC acts as an intermediate sandwich layer between the base metal and an aesthetic paint. Although chromate CCs offer superior performance compared to phosphate CCs, yet still they release carcinogenic hexavalent chromium ions (Cr^{6+}); therefore, their use is prohibited in most European nations under the Registration, Evaluation, Authorization and Restriction of Chemicals legislation framework. Phosphate-based CCs are a cost-effective and environment-friendly alternative. Accordingly, this review primarily focuses on different types of phosphate-based CCs, such as zinc, calcium, Mg, vanadium, manganese, and permanganate. It discusses their mechanisms, current status, pretreatment practices, and the influence of various parameters—such as pH, temperature, immersion time, and bath composition—on the coating performance. Some challenges associated with phosphate CCs and future research directions are also elaborated.

Keywords: phosphate conversion coatings; magnesium alloys; corrosion; zinc phosphate conversion coatings; calcium phosphate conversion coatings; magnesium phosphate conversion coatings

1. Introduction

Magnesium (Mg) and its alloys are used in different industries, including automotive, aerospace, electronics, and medical, due to their excellent properties, such as low density, high damping capacity, biocompatibility, machinability, high strength-to-weight ratio, castability, and weldability [1]. However, one of the major challenges associated with Mg and its alloys is their high susceptibility to corrosion even in neutral environments, thus limiting their widespread potential applications. Compared to other engineering structural materials, Mg has higher electrochemical activity, and it does not form a stable oxide layer on its substrate, unlike aluminum (Al) or titanium (Ti). The oxide films formed on Mg are mostly porous, inhomogeneous, and fragile, resulting in poor corrosion protection. Moreover, the reduction potential of Mg ($E^0_{Mg^{2+}/Mg}$ = −2.37 V vs. standard hydrogen electrode (SHE)) is significantly lower than those of other metals. Thus, in multi-material scenarios, Mg alloys are prone to galvanic coupling [2].

To overcome the challenges in corrosion, one of the widely accepted methods is to coat the underlying substrate. Several techniques, such as chemical conversion coating (CC), electroplating, anodizing, organic coating, hybrid coating, electroless coating, and vapor phase processes, are used to coat the Mg substrate [3]. Out of these, chemical CC is preferred in industries due to its favorable economics and operational simplicity. Different types of CCs, based on chromium, phosphate, rare earth, stannate, and vanadium, are used for Mg to prevent corrosion [4].

Chromium-based CCs (CCCs) exhibit excellent corrosion resistance and self-healing properties and are widely used in different industries. However, despite their superior performance, during the CCC process, hexavalent chromium ions (Cr^{6+}) are produced, which are harmful and carcinogenic and whose use is prohibited in most European nations [5–6]. Accordingly, the Registration, Evaluation, Authorization and Restriction of Chemicals (REACH) legislation was developed and enacted in the European Union in 2006 with the aim of preventing the usage of dangerous and toxic chemicals [7]. Under REACH, the application of hexavalent chromium compounds belonging to the Substances of Very High Concern category is currently under restriction. Trivalent chromate-based coatings, an alternate to CCCs, have been

✉ Corresponding author: Kisor K Sahu Email: kisorsahu@iitbbs.ac.in

studied to solve the toxicity problem. However, trivalent chromium ions (Cr^{3+}) lack self-healing capacity and produce a coating with inferior corrosion resistance [8]. Furthermore, there are some other concerns with existing coating technologies. For example, anodizing coatings have porosity issues, electroplated substrates are prone to galvanic corrosion, organic coatings have serious adhesion problems, and rare-earth-based CCs are highly expensive [9]. Thus, the need for alternative cost-effective CC techniques is essential to protect underlying substrates from the harsh environment.

Phosphate CCs (PCCs) were initially proposed for coating on steel substrates, and later on, this technique was adapted for the alloys of Al and Mg [10]. PCCs are generally more environmentally friendly than CCCs. Different PCCs have been reported in the literature depending on the metal cation source, such as zinc, calcium, zinc–calcium, Mg, manganese, permanganate, and molybdate [1,11]. Moreover, studies have revealed that the corrosion resistance of PCCs is comparable with that of CCCs [11–12].

In recent years, there have been several reviews on different types of CCs for Mg alloys. For instance, Saji [13] reviewed rare-earth-based CCs, such as lanthanum, yttrium, and cerium, for Mg alloys. Pommeirs *et al.* [11] discussed alternate non-chromate-based CCs, such as trivalent chromate, phosphate, vanadium, and permanganate. Zhang *et al.* [4] described physical barriers and smart healing coating techniques by emphasizing the need for smart healing coatings. Shadanbaz and Dias [14] reported the usage of calcium-based phosphate CCs for biomedical applications. Chen *et al.* [1] summarized different types of CCs, such as chromate, phosphate, fluoride, stannate, and rare-earth elements. However, there are still limited reviews available on broad-based phosphate CCs. In addition, pretreatment practices and their role on PCCs are yet to be studied. This review classifies different pretreatment procedures into two broad categories and discusses their implications on the corrosion performance of coatings. Moreover, emphasis has been given to different phosphate-based CCs and their mechanisms, applications, advantages, and limitations. This article critically analyzes some of the important aspects of PCCs, such as the influence of process parameters and bath additives, the role of surface defects, and the assessment of corrosion evaluation techniques.

2. Materials: Magnesium and its alloys

This review focuses on different types of Mg alloys, such as Mg–Al, Mg–Zr, and Mg–Li. The American Society for Testing and Materials (ASTM) alphanumeric designations are commonly used to distinguish different Mg alloys based on their composition. As per the ASTM standards, some of the commonly used Mg alloys are Mg–Al–Mn (AM), Mg–Al–Zn (AZ), Mg–Zn–Zr (ZK), and Mg–Zn–Li (LZ) [15], the details of these alloys are available in Table 1.

Table 1. Alloy compositions of different magnesium alloys wt%

Alloy	Mg	Al	Zn	Mn	Zr	Li
AZ31	Balance	3.0	1.0	0.2	—	—
AZ61D	Balance	6.3	0.7	—	—	—
AZ60	Balance	5.8–7.2	1	0.15–0.5	—	—
AZ80A	Balance	7.8	0.4	—	—	—
AZ91D	Balance	8.3–9.7	0.35–1.0	0.15–0.5	—	—
AM60	Balance	5.6–6.4	0.2	0.26–0.5	—	—
ZK60	Balance	—	5.5	—	0.5	—
LZ91	Balance	0.22	0.85	—	—	9.73

Some of the commonly used Mg–Al alloys are AZ91 and AZ31. The predominant phase in these alloys is the Mg matrix (α phase), whereas, depending on the concentration of Al in the Mg alloy, the intermetallic particles $Mg_{17}Al_{12}$ and AlMnSi constitute the β phase. Fig. 1 [16] shows the optical micrographs of the AZ31 and AZ91 alloys consisting of α and β phases. Evidently, the β phase is more prominent in AZ91 than AZ31 which makes the surface electrochemically non-uniform. In Mg–Al alloys, due to higher corrosion potential, the β phase acts as the cathode while the α phase behaves as an anode. Moreover, few studies have found that the β phase plays a vital role in increasing the corrosion performance of conversion coated substrates [17].

3. Conversion coating overview

CCs are used in different industries to protect bare substrates from corrosion and to increase the adhesion of the topcoat. The usage of CC increases paint adhesion, which makes the CC process critical in many industries [10]. PCC is a widely studied technique due to its low cost and less toxicity. The preparation of PCC and its corrosion investigation consists of different steps, as shown in Fig. 2. The first step is the pretreatment, where different processes, such as polishing, alkaline degreasing, and acid pickling, are performed before the PCC process to enhance the coating deposition. The second step is the CC process, where insoluble precipitates are deposited on the substrate due to an increase in pH near the vicinity of the specimen. To investigate the corrosion behavior of coating, various techniques are used: for surface morphology analysis —X-ray diffraction (XRD), scanning electron microscopy (SEM), energy-dispersive spectroscopy/X-ray analysis (EDS/EDX), and X-ray photoelectron spectroscopy (XPS); for corrosion studies—electrochemical impedance spectroscopy (EIS), potentiodynamic polarization (PDP), hydrogen evolution, salt spray, and adhesion test. The

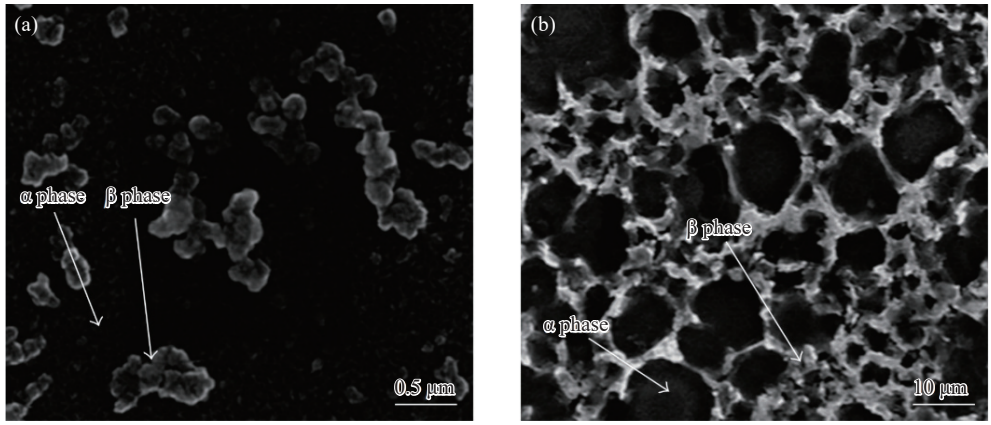

Fig. 1. Surface morphologies demonstrating the α and β phases in (a) AZ31 and (b) AZ91 [16]. AZ91 contains more β phase, which at times facilitates the CC and makes the surface heterogeneous (see text for details).

quality, compactness, and corrosion resistance of the final PCCs are influenced by pH, temperature, phases and microstructure, alloy constituents, pretreatment practices, bath composition, type of additives, and immersion time. The role of different types of additives, such as sodium dodecyl sulfate (SDS), mono-ethanolamine (MEA), and triethanolamine (TEA), on the corrosion protection of PCCs, is discussed in this article. Further details regarding CCs can be found elsewhere [1,3,18].

The mechanism of PCCs in Mg alloys is described in Fig. 3. The initial step of a PCC process is electrochemical in nature. Upon immersion in the acidic phosphate bath, the dissolution of Mg occurs at the α phase (anode), and simultaneously H^+ ions reduce to form H_2 gas at the β phase (cathode), which is shown in reactions (1) and (2), respectively. This redox reaction leads to an increase in the local pH and Mg^{2+} concentration in the vicinity of the alloy substrate. The rise in pH near the substrate makes the solubility product of the metal phosphate lower, thus facilitating precipitate deposition on the Mg alloy. Usually, the solubility limit of metal phosphates decreases with the increase in pH, thus contributing to precipitate formation. For example, in the case of a divalent cation-based (e.g., Ca^{2+}, Zn^{2+}, and Mg^{2+}) phosphate CC, upon reaching the requisite pH near the surface, respective insoluble metal phosphates precipitate on the substrate to protect the Mg alloy, as shown in Fig. 3.

$$Mg \rightarrow Mg^{2+} + 2e^- \quad (1)$$

$$2H^+ + 2e^- \rightarrow H_2 \quad (2)$$

At this point, the difference between the PCC (subject of this review) and some other coating mechanisms, for instance, plasma electrolytic oxidation (PEO) and anodizing, should be emphasized. PEO and anodizing are basically controlled electrolytic oxidation processes, where Mg acts as an anode. In a PEO process, a high potential of more than 200 V is applied. Usually, PEO and anodizing are preferred for aluminum alloys as the oxides of Al are more stable than those of Mg. The coatings formed by PEO and anodizing have

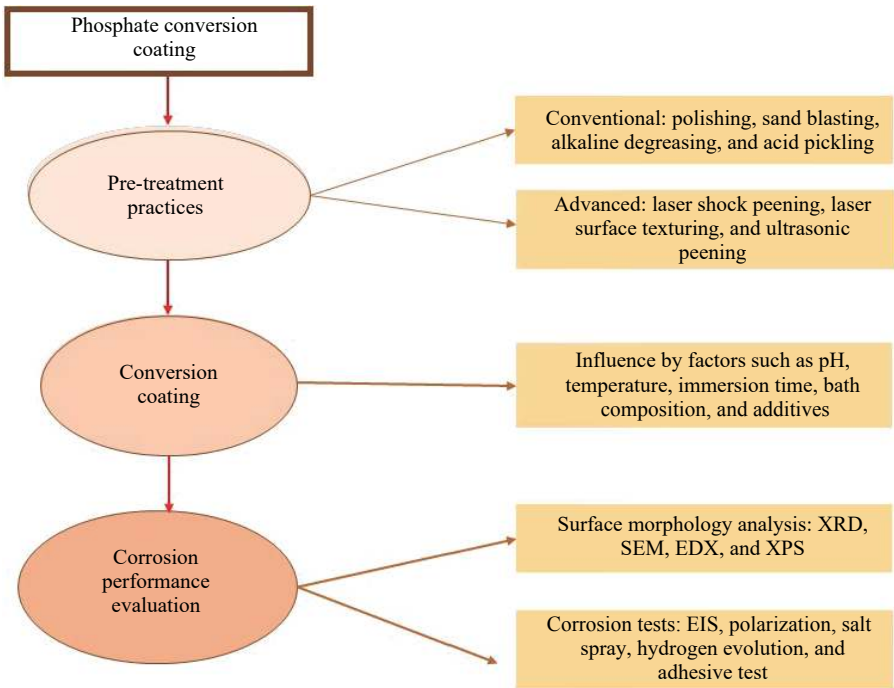

Fig. 2. Schematic of different steps in a phosphate conversion coating.

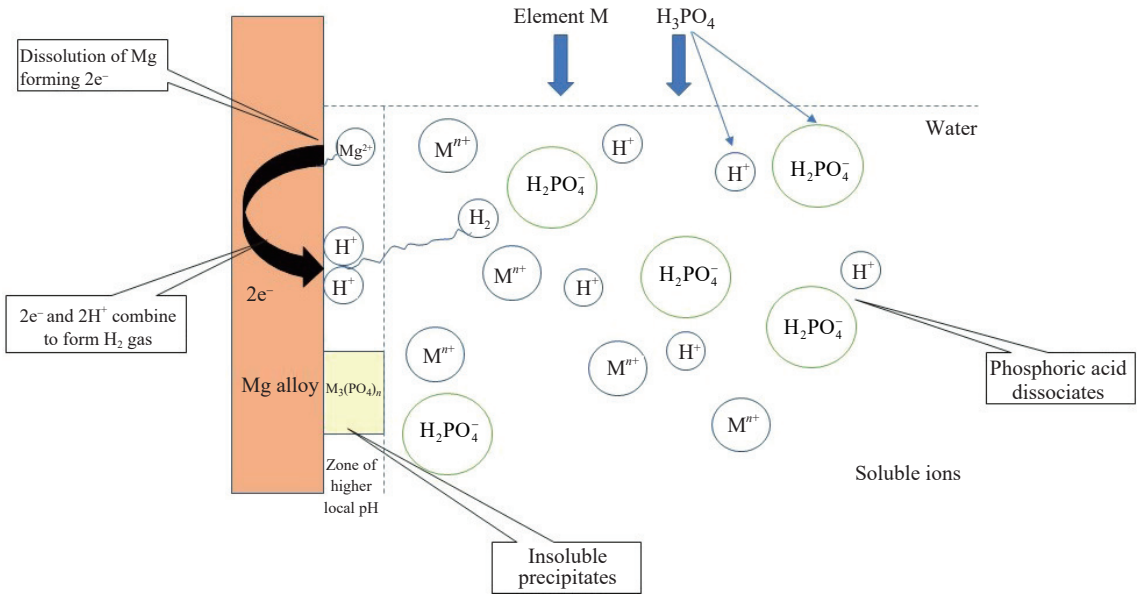

Fig. 3. Schematic describing the mechanism of phosphate conversion coating.

porosity issues. However, Pezzato *et al.* [19] developed two types of PEO coatings (PEO-Si and PEO-P) using different electrolytes on the AZ91 Mg alloy and reported a 90% reduction in the corrosion current density for the PEO-P coating over the bare substrate.

4. Pretreatment for phosphate CCs

The role of the pretreatment process is of critical importance in the development of successful coating technology. The pretreatment process brings many challenges in heterogeneous and aluminum-rich Mg alloys, such as AZ91D, due to the unequal distribution of aluminum, which ultimately results in the non-uniform growth of coating on the Mg substrate. The main objectives of pretreatment procedures before PCC are to increase the surface roughness, remove the Al-rich β phase, and tailor the cathodic/anodic character of the surface. Surface roughness plays a pivotal role in controlling the coatings' deposition rate and adhesion. High surface roughness increases the number of nucleation sites and interlocking forces, which leads to a high deposition rate and adhesion of coatings [20–21]. However, high surface roughness increases the porosity of coatings; thus, optimal roughness is desired for coating substrates [22]. The presence of the β phase makes the surface electrochemically heterogeneous, resulting in a non-uniform coating deposition. The pretreatment procedures are broadly classified into two categories: conventional techniques, which include acid pickling, alkaline conditioning, shot peening, sandblasting, and polishing, and advanced methods, comprising laser shock peening (LSP), laser texturing, and ultrasonic impact peening.

4.1. Conventional pretreatment approaches

Different pretreatment procedures for the surface activation of Mg and its alloys have been reported in the literature, and studies indicate that pretreated coated samples exhibit superior corrosion performance. Sandblasting, polishing, and grinding are basic mechanical pretreatment methods of removing surface contaminants, making the surface smooth, and altering surface morphology. Surface activation/acid pickling is performed to remove the oxide/hydroxide layer on the Mg substrate and to increase surface roughness. Alkaline degreasing is performed to clean the surface and remove the Al-rich β phase present in the Mg alloy.

Zhang *et al.* [23] studied the role of various pretreatment processes, i.e., sandblasting and polishing, on the AZ91 alloy. The surface roughness of the sandblasted sample was found to be higher than that of the polished specimen. A dense and uniform manganese phosphate CC (Mn-PCC) was formed on the polished AZ91 substrate. However, the sandblasted Mn-PCC resulted in a non-uniform and porous microstructure mainly because of the galvanic corrosion effect between the α Mg and the newly introduced β phase.

Li *et al.* [24] investigated the effect of pre-activators, such as oxalic acid (0.2wt%), colloidal Ti phosphate (5wt%), and phosphoric acid (10vol%), on the corrosion resistance of Mg–6.0Zn–3.0Sn–0.5Mn (ZTM630) Mg alloy at room temperature for a period of 20 s. The phosphoric acid pretreated coated sample exhibited the highest corrosion resistance with a corrosion potential (E_{corr}) of −1.347 V, an increase of approximately 15% over the bare substrate. They found that in all the samples, the obtained final phase was of the same phosphate compound, but the growth rate and surface morphology were different. Yang *et al.* [25] discussed different combinations of chemicals for alkaline conditioning and acid activation techniques for pretreatment and found that the treatment time and temperature of the solution play a critical role in dissolving the protruded β phase from the AZ91D alloy. They reported that a combination of citric acid and NaOH was optimal.

4.2. Advanced pretreatment approaches

Laser is a cost-effective surface modification tool for enhancing corrosion, wear resistance and hardness, among oth-

ers, of an underlying surface. Unlike chemical pretreatment techniques, laser-based procedures are environment-friendly. Recently, laser-based surface modification techniques have been used in the pretreatment process of Mg alloys to alter the surface morphology, corrosion resistance, and electrochemical activity of surfaces.

LSP induces several crystal defects (e.g., dislocations and twins), refines the grain structures, and produces compressive residual stresses at the surface layer [26–27]. Zhang *et al.* [28] reported that due to LSP, local plastic deformation occurs, which causes an increase in the grain refinement, dislocation, and twin density, ultimately improving the electrochemical activity of the surface. Thus, this process increases the number of nucleation sites for phosphate nuclei to grow. Residual compressive stress and refined grain structure on the surface layer act as a corrosion barrier, thereby reducing the corrosion rate. Laser surface texturing (LST) is a surface modification tool that produces multimodal roughness [29–30]. The main reason for the generation of multimodal roughness is that the substrate undergoes local heating, ablation, and rapid cooling multiple times in a short period, which improves the coating deposition, and the presence of grooves enhances adhesion [30].

Liu *et al.* [31] discussed the influence of LSP on the AZ31 Mg alloy by preparing four different samples, i.e., bare substrate, LSP, PCC, and LSP–PCC. The highest impedance and lowest corrosion current density (i_{corr}) were observed for the LSP–PCC. The surface morphology of the corroded samples revealed that LSP–PCC was the least affected. Jana *et al.* [9] studied the effect of a novel laser surface processing on the corrosion behavior of AZ31 alloy using a combination of low pulse energy (128, 234, and 312 mJ) and small laser spot size (500 μm). The laser surface-processed specimen with the following laser parameters (power setting 3.12, pulse energy 312 mJ, and beam spot size 500 μm) exhibited the highest corrosion resistance.

Liu *et al.* [30] developed a surface modification technique for increasing the corrosion resistance of the AZ31 alloy using a combination of LST and PCC. They reported that the surface roughness and specific area significantly increased after the LST procedure. They found that with LST, i_{corr} reduced by approximately three times over the bare substrate. As shown in the EDS mapping (Fig. 4), the LST pretreatment did not alter the distribution of coating elements.

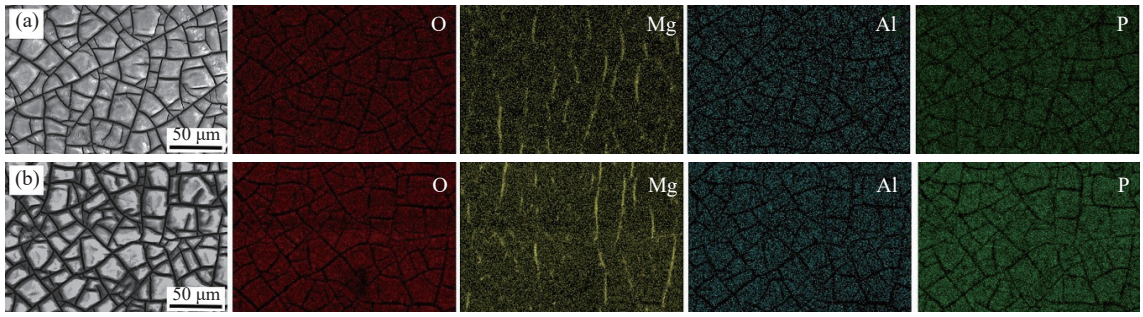

Fig. 4. EDS mapping of PCC consisting of P, Mg, Al, and O: (a) ARC (as-received coating) sample and (b) LTC (coating with the LST pretreatment) sample [30]. Reprinted from *J. Alloys Compd.*, 865, H.L. Liu, Z.P. Tong, Y. Yang, W.F. Zhou, J.N. Chen, X.Y. Pan, and X.D. Ren, Preparation of phosphate conversion coating on laser surface textured surface to improve corrosion performance of magnesium alloy, 158701, Copyright 2021, with permission from Elsevier.

5. Types of phosphate CCs

In recent years, the demand for Mg and its alloys has been rising in various sectors, such as automobile, aerospace, medical, and electronics. However, Mg alloys are prone to corrosion, so PCCs have become one of the alternatives to meet industrial requirements. Different PCCs for Mg alloys have been developed depending on specific requirements [32]. For example, zinc phosphate CCs (Zn-PCCs) and rare-earth coatings are thermally stable, so they are useful for high-temperature applications, unlike their chromate-based alternatives [11,13]. Zn-PCCs are used as a base layer/coat prior to painting in automobile outer bodies to increase paint adhesion [10]. Lanthanum phosphate (La-P) coatings find utility in producing ceramic crucibles for casting in high-temperature applications [33]. Moreover, the compounds formed during calcium- and Mg-based PCCs are biocompatible, and hence, they are applicable in human body implants and bone fixation, among others [14]. Furthermore, during Mn-based coatings, $Mn_3(PO_4)_2$ precipitates are formed, which are lubricating in nature and find utility in gears, bearings, and the oil and gas industry. Accordingly, this section primarily discusses different types of phosphate-based coatings, their applications, demerits, and mechanisms in detail.

5.1. Zinc phosphate

Zn-PCCs on Mg substrates are one of the most extensively studied techniques to protect underlying materials. The major advantages of Zn-PCCs are lower toxicity and better corrosion resistance at high temperatures, as compared with CCC. Moreover, Zn-PCCs improve the paint adhesion of coatings compared to bare substrates. The main phase present in the microstructure of Zn-PCCs is hopeite ($Zn_3(PO_4)_2 \cdot 4H_2O$). The zinc phosphate bath consists of a Zn^{2+} ion source, PO_4^{2-} source, accelerators, inhibitors, and other suitable reagents. Some reported bath compositions, coating characteristics, and corrosion studies are described in Table 2 [34–37].

In a Zn-PCC, when the Mg alloy is immersed in the zinc

Table 2. Bath composition and coating characteristics of the zinc phosphate conversion of coatings

Alloy	Bath composition	Process parameter			Coating characteristics & composition	E_{corr} / V	i_{corr} / (mA·cm^{-2})	Ref.
		pH	Temp. / °C	Immersion time / min				
AZ31	$Zn(NO_3)_2·6H_2O$: 5 g/L; NaF: 1 g/L; $NaNO_2$: 3 g/L; $NaNO_3$: 1.84 g/L; H_3PO_4: 7.4 mL; $NaH_2PO_4·12H_2O$: 20 g/L	3	80	10	Crystalline flakes like structure; $Zn(PO_4)_2·4H_2O$ (outer layer, hopeite)	n.d.	0.494	[34]
AZ31	ZnO: 3.2 g/L; NaF: 1.7 g/L; tartaric acid: 2.4 g/L; H_3PO_4: 10 mL/L; SDS: 0.8 g/L	1.9–2.1	45–50	5	Uniform and denser coating with fewer micro-cracks; $Zn(PO_4)_2·4H_2O$ (outer layer, hopeite)	−1.422	0.03301	[35]
AZ91D	ZnO: 6.8 g/L; H_3PO_4: 27.2 g/L; NaF: 1.2 g/L; MEA: 1.2 g/L; $C_4H_6O_6$: 2.2 g/L; accelerator: 4.9 g/L	2.8–3.3	45	10	Inner layer consists of micro cracks; outer layer mainly hopeite	−1.29	0.9×10^{-3}	[37]
AZ91D	ZnO: 2.2 g/L; H_3PO_4: 11.3 g/L; NaF: 2.3 g/L; organic amine: 1.2 g/L; zinc nitrate: 12.5 g/L; complex accelerator: 1.6 g/L	2.2–2.4	20 & 45	5	Coating composed of $Zn(PO_4)_2·4H_2O$ and $AlPO_4$	n.d.	n.d.	[36]

Note: Temp.—Temperature; Ref.—Reference; n.d.—No data.

phosphate bath, the dissolutions of Mg and H_2 evolution occur spontaneously in accordance with reactions (1) and (2), respectively. These reactions result in the generation of H_2 bubbles, which increase the pH level around the substrate. The rise in the local pH near the vicinity of the substrate favors the precipitation of insoluble hopeite in accordance with reaction (3):

$$3Zn^{2+} + 2H_2PO_4^- + 4H_2O \rightarrow Zn_3(PO_4)_2 \cdot 4H_2O + 4H^+ \quad (3)$$

Moreover, nitrate ion-based accelerators (oxidizing agents) are used to increase the dissolution rate of Mg, which enhances the precipitation rate of hopeite in accordance with reaction (4).

$$Mg + NO_3^- + 2H^+ \rightarrow Mg^{2+} + NO_2^- + H_2O \quad (4)$$

The temperature of the Zn-PCC bath plays a critical role in deciding the coating deposition quality on Mg alloys. Cheng *et al.* [34] reported that coatings formed at 80°C with an immersion time of 10 min exhibited the highest corrosion resistance. The XRD patterns of the coated surface confirmed the presence of hopeite with a flake-like crystalized structure. The increase in the temperature of the coating bath decreased the immersion time. This is primarily because at high temperatures, the activation energy of the phosphating process is low. Thus, the rate of the phosphate reaction is increased, and a compact coating is formed on the Mg substrate.

SDS is an anionic surfactant that increases the number of micro-cathode sites during CC, as shown in Fig. 5. SDS molecules, which are anionic in nature, are absorbed into micro-anode sites (with a low electron density) and increase the electron density of micro-anode sites, thus enabling them to act as micro-cathode sites. Amini and Sarabi [35] found that an increase in the SDS concentration increased the corrosion resistance in the AZ31 Mg alloy. The presence of uniform and low micro-cracks on coatings resulted in flake-like denser morphologies. They suggested that by using SDS, the number of micro-cathode sites can be increased, which ultimately increased the rate of phosphate CCs.

Niu *et al.* [36] studied the effect of accelerators (alkyl phosphate salt, hydrogen peroxide, and a complex mixture of sodium cerium and sodium chlorate) in Zn-PCC baths on the AZ91D Mg alloy. They found that the optimum complex accelerator, i.e., sodium cerium and sodium chlorate (in a mass ratio of 1:25), exhibited good corrosion resistance. Phuong *et al.* [38] studied the effects of the Zn^{2+} ion concentration and pH for evaluating the corrosion performance in Zn-PCCs. They investigated nine different iterations of Zn^{2+} and pH based on the predominance diagram of zinc phosphate. They found that a zinc concentration of 0.068 M at pH 3.07 yielded the best corrosion results.

Li *et al.* [37] found that a bath containing 1.2 g/L of the inhibitor MEA exhibited the highest corrosion resistance for the AZ91D Mg alloy. They observed that i_{corr} was 0.9×10^{-3} mA/cm^2, which is approximately 99.4% lower than that of the bare substrate. The coating was duplex in nature, i.e., a crystalline outer layer (hopeite) and an amorphous inner layer (oxides of Mg with cracks). The corrosion efficiency of bare AZ91D can also be increased upon immersion in a solution containing inhibitors. For instance, Shang *et al.* [39] found that a concentration of 3 mL/L TEA showed the highest inhibition efficiency (91.97%) in 3.5wt% NaCl for an immersion time of 1 h. The adsorption studies found that the adsorption of TEA molecules followed the Langmuir adsorption isotherm equation and that at a low temperature (20°C), the standard adsorption equilibrium constant (K_{ads} = 3333.33) was the highest.

5.2. Calcium phosphate

The calcium phosphate CC (Ca-PCC) process is an extensively studied coating technique for biomedical applications on Mg alloys [14,40]. It has been found that 70% of nat-

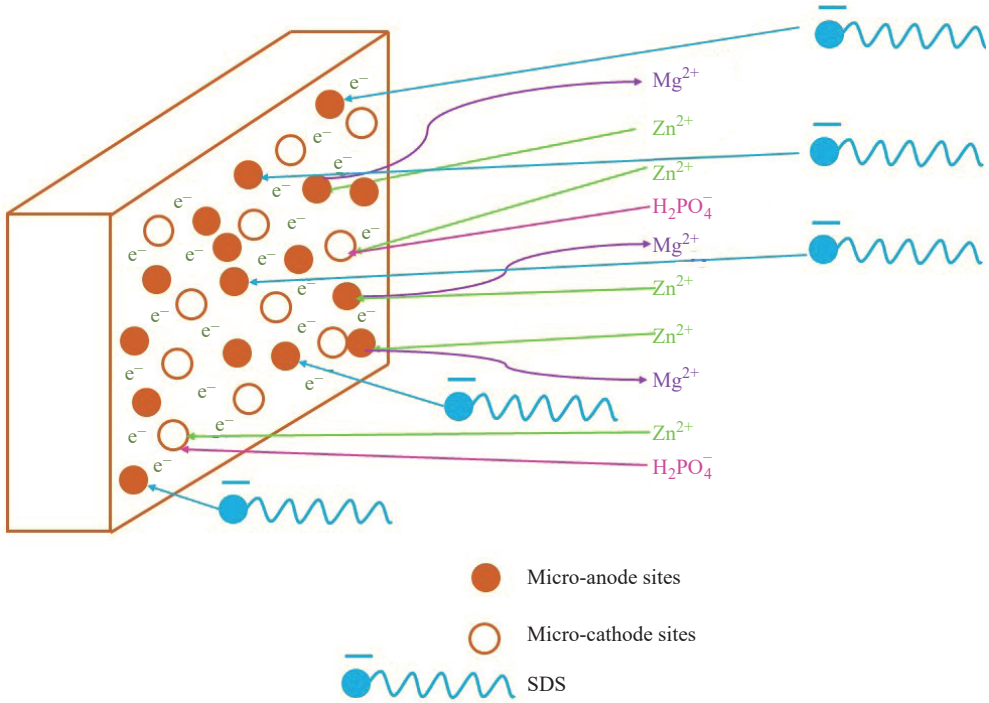

Fig. 5. Schematic demonstration of the influence of SDS on the coating creation of the AZ31 Mg alloy [35]. Reprinted from *Appl. Surf. Sci.*, 257, R. Amini and A.A. Sarabi, The corrosion properties of phosphate coating on AZ31 magnesium alloy: The effect of sodium dodecyl sulfate (SDS) as an eco-friendly accelerating agent, 7134-7139, Copyright 2011, with permission from Elsevier.

ural bone tissues are made up of calcium phosphate, thus making the Ca-PCC process a suitable coating technique for human body implants [32]. During the Ca-PCC process, different compounds/precipitates are formed on the Mg substrate, such as dicalcium phosphate dihydrate (DCPD, $CaHPO_4{\cdot}2H_2O$), Mg hydrogen phosphate trihydrate (MHPT, $MgHPO_4{\cdot}3H_2O$), hydroxyapatite (HA, $Ca_{10}(PO_4)_6(OH)_2$), and Mg whitlockite (MWH, $Ca_9Mg(HPO_4)(PO_4)_6$) [41]. The products HA and DCPD are biocompatible and are used in human body implants [42].

Upon immersion of Mg in a Ca-PCC bath, due to reactions (1) and (2), the local pH and Mg^{2+} ion concentration in the vicinity of the metal surface increases. The increase in Mg^{2+} promotes the formation of MHPT as per reaction (5). The Ca^{2+} ions interact with phosphate ions forming DCPD as per reaction (6). The formation of MWH takes place due to the simultaneous occurrence of Mg^{2+} and Ca^{2+} ions on the Mg surface, which is described in reaction (7). The precipitates of MHPT, MWH, and DCPD are formed only when the local pH rises enough to exceed their solubility limit.

$$Mg^{2+} + H_2PO_4^- + 3H_2O \rightarrow MgHPO_4 \cdot 3H_2O + H^+ \quad (5)$$

$$Ca^{2+} + H_2PO_4^- + OH^- + H_2O \rightarrow CaHPO_4 \cdot 2H_2O \quad (6)$$

$$9Ca^{2+} + Mg^{2+} + 7H_2PO_4^- + 13OH^- \rightarrow Ca_9Mg(HPO_4)(PO_4)_6 + 13H_2O \quad (7)$$

Su *et al.* [43] studied Ca-PCCs on the AZ60 Mg alloy for biomedical applications. They reported that at pH value of 2.8–3.0 and temperature of 37°C provide excellent corrosion resistance. They observed that three layers of CCs were formed. The inner layer consisted of MHPT, whereas the middle layer was composed of DCPD, MHPT, and MWH. The outer layer consisted of MWH and DCPD with a thickness of 2.3 µm. Amaravathy and Kumar [44] discussed a novel strontium-based zinc calcium phosphate CC (SZCP) for biomedical applications on an AZ31 Mg alloy. The corrosion behavior of the coated samples was studied in a simulated body fluid (SBF) solution using a hydrogen evolution test. They found that the corrosion resistance of SZCP was superior in comparison to the conventional zinc–calcium phosphate coating (Zn–Ca-PCC). Zai *et al.* [45] studied seven different types of chemical CCs (can be broadly classified into three types: Mg-PCCs, Zn-PCCs, and Ca-PCCs) for evaluating the corrosion performance and biocompatibility of the AZ31 Mg alloy. The Cell Counting Kit 8 (CCK-8) tests were performed to determine the biocompatibility of coated AZ31 samples. They found that Ca-PCCs performed better in the biocompatibility test than Mg-PCCs. Guo *et al.* [46] investigated the biocompatibility of a composite coating made up of calcium phosphate (Ca-P) and collagen (Col) on the AZ60 Mg alloy. The cracks and pores of Ca-P coating were sealed efficiently by collagen coating, thus significantly increasing the corrosion protection of the alloy. Moreover, the composition of the Ca-P/Col coating was similar in nature to that of bone, therefore increasing the biocompatibility of these types of coatings to a great extent.

Liu *et al.* [47] found that Ca-P-coated samples consisted of leaf-like structures composed of DCPD with few cracks and pores. Their study revealed that increasing the immersion time from 5 to 20 min resulted in the formation of compact and dense coatings, but at an immersion time of 25 min, less sparse coatings were obtained (as shown in Fig. 6). The optimal coating was found at ambient temperature, pH value of 2.8, and immersion time of 20 min. Chen *et al.* [48] found

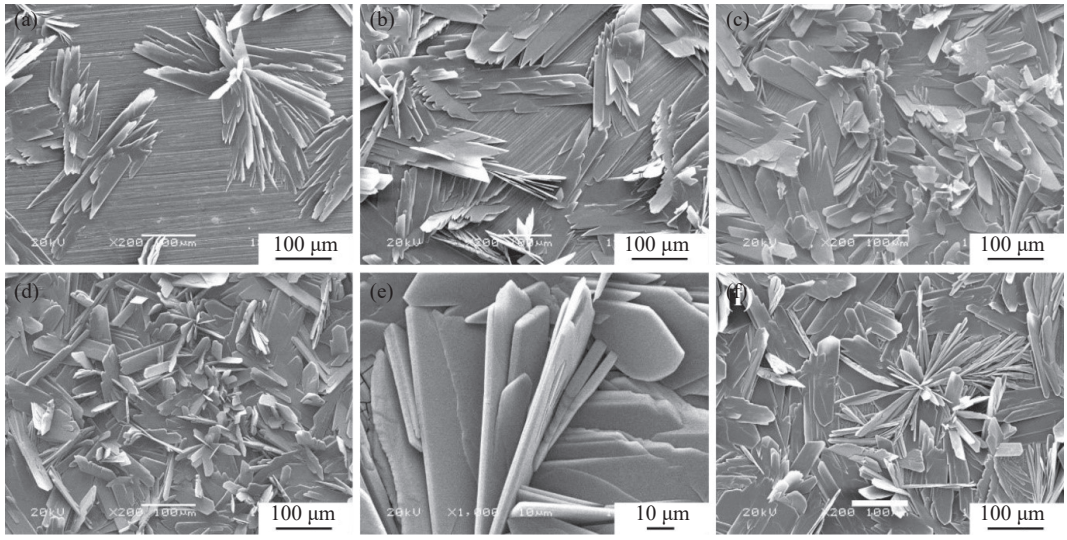

Fig. 6. Surface morphologies of Ca-PCCs at different immersion times: (a) 5 min; (b) 10 min; (c) 15 min; (d) 20 min; magnification of (e) 20 min and (f) 25 min [47].

that the coating with a high Ca^{2+} concentration (10 mM) and low PO_4^{2-} concentration (1 mM) exhibited the highest corrosion protection on the AZ91D Mg alloy. Further details regarding the bath compositions can be found in Table 3 [43,46–50].

5.3. Magnesium phosphate

Mg phosphate CCs (Mg-PCCs) were initially used to coat the substrates of other structural materials, such as steel [51], and are currently used for protecting Mg substrates against corrosion. It is one of the promising alternatives to Zn-PCCs and Ca-PCCs. Mg-PCCs perform better in salt spray tests in comparison to other types of CCs [52–53]. The details of the different bath compositions of Mg-PCCs are discussed in Table 4 [42,52,54–56].

When Mg was immersed in a phosphate coating bath, due to an increase in the local pH near the metal surface, different compounds/precipitates were deposited on the substrate according to reactions (8)–(12). The microstructure of Mg-PCCs mainly consists of the phases of farringtonite/Mg phosphate ($Mg_3(PO_4)_2$), newberyite/berryite/MHPT ($MgHPO_4{\cdot}3H_2O$), and struvite ($MgNH_4(PO_4){\cdot}6H_2O$). The source of phosphate ions decides the phases and microstructure of Mg-PCCs, assuming that the local pH is optimum for the precipitate formation. For example, when phosphoric acid (H_3PO_4) is used as a phosphate ion source, basically, the observed phases are newberyite and Mg phosphate as per reactions (8) and (9). By contrast, with ammonium dihydrogen phosphate, the presence of all the three phases, i.e., struvite, newberyite, and Mg phosphate, is possible according to reactions (10)–(12). These precipitates are formed only when

Table 3. Bath composition and coating characteristics of the calcium phosphate conversion of coatings

Alloy	Bath composition	Process parameter			Coating characteristics & composition	Coating thickness / μm	E_{corr} / V	i_{corr} / (μA·cm^{-2})	Ref.
		pH	Temp. / °C	Immersion time / min					
AZ60	$Ca(NO_3)_2{\cdot}4H_2O$: 12 g/L; CaO: 1.2 g/L; H_3PO_4 (85vol%): 8 mL/L	2.8	n.d.	20	Duplex coating layer having dense inner layer (MHPT) and porous outer layer (DCPD & MWH)	3.9	n.d.	n.d.	[43]
AZ60	$Ca(NO_3)_2{\cdot}4H_2O$: 23.6 g/L; H_3PO_4: 34.2 mL/L	2.8	37	10	Flake-like structure having a composition (Ca-P/Col) similar to bone so acting as a biocompatible coating	10	−1.23	0.87	[46]
AZ91D	$Ca(NO_3)_2{\cdot}4H_2O$: 25 g/L; $NH_4H_2PO_4$: 15 g/L	2.8	40	20	Leaf-like coating having composition $CaHPO_4{\cdot}2H_2O$	n.d.	−1.493	0.61	[47]
AZ91D	$Ca(NO_3)_2$: 25 g/L; $NH_4H_2PO_4$: 25 g/L	3	40	5	Coating having composition HA and DCPD making it biocompatible due to its stable and inert composition	n.d.	−1.18	n.d.	[48]
AZ31	Na_2HPO_4: 10 g/L; $Zn(NO_3)_2$: 6 g/L; $Ca(NO_3)_2$: 2 g/L; $NaNO_2$: 4 g/L; NaF: 2 g/L	2.5	55	20	Dense coating with flower-like morphology with few cracks of composition $Zn_3(PO_4)_2{\cdot}4H_2O$ (hopeite) and ZnO	n.d.	−1.498	11.5	[49]
AZ91D	$NH_4H_2PO_4$: 0.2 M; $Ca(NO_3)_2$: 0.1 M; $NaVO_3$: 0.08 M	3	40	20	Coating having a grid-like structure with self-healing capability having a large number of micro-cracks	n.d.	−1.45	0.384	[50]

Table 4. Bath composition and coating characteristics of the magnesium phosphate conversion of coatings

Alloy	Bath composition	Process parameter			Coating characteristics & composition	Coating thickness / μm	E_{corr} / V	i_{corr} / (μA·cm^{-2})	Ref.
		pH	Temp. / °C	Immersion time / min					
AZ31	$NH_4H_2PO_4$: 1 mol/L	7.5	50	20	Dense and continuous coating of fine phosphate crystals having composition struvite ($MgNH_4PO_4·6H_2O$) and newberyite ($MgHPO_4·3H_2O$)	32–35	−1.53	9.02	[55]
AZ31	H_3PO_4: 0.24 mol/L; Mg $(OH)_2$: 0.1 mol/L	n.d.	n.d.	20	Having better corrosion resistance with paint as compared to Zn-PCCs. Coating composition includes $MgHPO_4·3H_2O$, $Mg_3(PO)_2$, and $Mg(OH)_2$	3	−1.44	6.3	[52]
AZ31	$Mg(NO_3)_2$: 0.4 mol/L; H_3PO_4: 0.2 mol/L	2.7	60	20	Continuous coating of grain size 5 μm of composition newberyite ($MgHPO_4·3H_2O$)	17	−1.544	0.206	[45]
AZ31	$Mg(OH)_2$: 0.1 mol/L; H_3PO_4: 0.24 mol/L	n.d.	45	20	Uniform coating with some micro-cracks on the surface having composition MgO/$Mg(OH)_2$ and Mg-phosphate	2.5	−1.41	6.9	[56]
AZ31	H_3PO_4: 0.34 mol/L; $Mg(NO_3)_2$: 0.35 mol/L	3	80	10	Duplex layered coating having fine equiaxial crystal of composition $MgHPO_4·3H_2O$	32–41	n.d.	n.d.	[54]

their solubility limit is exceeded due to an increase in the local pH.

$$Mg^{2+} + H_2PO_4^- + 3H_2O \rightarrow MgHPO_4 \cdot 3H_2O + H^+ \quad (8)$$

$$3Mg^{2+} + 2PO_4^{3-} \rightarrow Mg_3(PO_4)_2 \quad (9)$$

$$NH_4H_2PO_4 \rightarrow NH_4^+ + H_2PO_4^- \quad (10)$$

$$Mg^{2+} + H_2PO_4^- + 3H_2O \rightarrow MgHPO_4 \cdot 3H_2O + H^+ \quad (11)$$

$$Mg^{2+} + H_2PO_4^- + NH_4^+ + 6H_2O \rightarrow MgNH_4PO_4 \cdot 6H_2O + 2H^+ \quad (12)$$

The pH and temperature of the Mg-PCC bath play a critical role in the quality of the coating. Based on a report, at 80°C and pH = 3.0, the corrosion resistance is the highest in comparison to other temperature–pH combinations [54]. Jayaraj *et al.* [55] found that at pH = 4.5, maximum coating thickness (48 μm) was obtained on the AZ31 substrate. The composite Mg-PCC consisted of newberyite and struvite phases. They found that with an increase in pH, the coating performance increased due to the presence of more insoluble struvite particles.

Few studies have demonstrated that Mg-PCC performed better in salt spray and adhesion tests in comparison with Zn-PCC. For example, van Phuong *et al.* [52] studied the performance of Mg-PCC and Zn-PCC and found that Mg-PCC samples were more resilient to salt spray and adhesion tests, thus making them a viable alternative against conventional Zn-PCC. Fouladi and Amadeh [53] found that an Mg-PCC specimen was approximately three times thicker than Zn-PCC. They observed that Mg-PCC samples can withstand the corrosive environment 100 h more than the Zn-PCC specimens in salt spray tests.

Similar to Ca-PCC, Mg-PCC has also been reported for biomedical applications. Zai *et al.* [54] reported an Mg-PCC to enhance corrosion resistance on the AZ31 Mg alloy used for human implant materials. The microstructures of coated samples revealed the presence of phase $MgHPO_4·3H_2O$ in the inner layer and precipitated crystalline outer layer. The inner layer contributed to improving the corrosion resistance. They found that for optimal coating, E_{corr} and i_{corr} were −1.51 V vs. SCE (i.e., saturated calomel electrode) and 57 nA/cm^2, respectively, and were carried out in Hanks' balanced salt solution (SBF). However, a study by Zai *et al.* [45] revealed that the corrosion behavior of Mg-PCC for bio-implant applications was lagging in comparison to other PCCs. The CCK-8 tests were performed to determine the biocompatibility and found that the cell viability of calcium-based phosphate coatings was better than that of Mg-PCC. Thus, further studies are needed to explore the usage of Mg-PCC in human body implants.

5.4. Manganese phosphate

Manganese phosphate CC (Mn-PCC) was initially used to enhance the tribological properties of high-strength steel applications. The major disadvantages of Zn-PCCs are high porosity, inferior thermal properties, and non-uniform crystal structure [32]. Considering these demerits, recently, Mn-PCC has been used for enhancing the surface characteristics of Mg alloys. In the Mn-PCC, when the Mg metal/alloy was inserted into the coating bath, the dissolution of Mg occurred inside the bath, followed by the deposition of the $Mg(OH)_2$/MgO film forming the intermediate layer, and finally a layer of $Mn_3(PO_4)_2$ was precipitated in accordance to reaction (13). The formation of $Mn_3(PO_4)_2$ (having better lubrication properties) depends on various parameters, such as temperature, pH, and immersion time.

$$4Mn^{2+} + 3H_2PO_4^- \rightarrow MnHPO_4 + Mn_3(PO_4)_2 + 5H^+ \quad (13)$$

Zhou *et al.* [57] reported that the presence of α and β phases in the Mg alloy (AZ91D) was responsible for the formation of Mn-PCC. During the Mn-PCC process, the α phase (anode) from where the dissolution of Mg^{2+} ions occurs and the β phase (cathode) where H_2O is reduced and hydrogen gas evolves. Due to the presence of OH^- ions in the vicinity of the cathode site, the pH value increased, resulting in the deposition of manganese dihydrophosphate precipit-

ates on the substrate. Moreover, flower-like (relatively thinner) and ball-like precipitations occur at the β and α phases, respectively.

Zhou *et al.* [58] investigated the influence of additives, such as fluoride and organic acid (phytic acid), on Mn-PCC and found that these additives increased the corrosion resistance. They found that the film became more compact and uniform, consisting of smaller grains, which reduced the substrate area exposed to the environment. The E_{corr} for fluoride bath, phytic bath, and conventional bath were −139, −179, and −187 mV vs. SCE, respectively. Cui *et al.* [59] studied the role of additives, such as sodium fluoride (NaF), sodium citrate ($C_6H_5Na_3O_7$), and citric acid ($C_6H_8O_7$). The bath containing citric acid exhibited the highest E_{corr}, followed by NaF and sodium citrate, as shown in Fig. 7. The primary reason for the increase in the E_{corr} of the citric bath is the formation of a duplex layer of coating on the metal substrate. However, the coating formed is crystalline in nature and composed of a lamellar and block structure, which is not consistent with the coating formed by Zhou *et al.* [57] that has an amorphous characteristic.

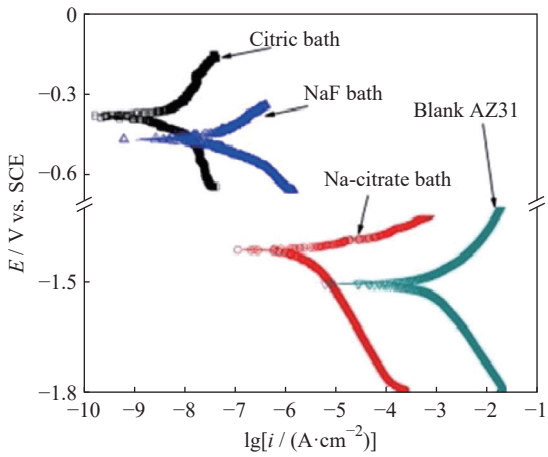

Fig. 7. Potentiodynamic polarization of different phosphate baths and bare AZ31 alloy in 3.5wt% NaCl [59]. Reprinted from *Corros. Sci.*, 76, X.J. Cui, C.H. Liu, R.S. Yang, Q.S. Fu, X.Z. Lin, and M. Gong, Duplex-layered manganese phosphate conversion coating on AZ31 Mg alloy and its initial formation mechanism, 474-485, Copyright 2013, with permission from Elsevier.

Cui *et al.* [60] studied the effect of pH and temperature and found that high temperatures favor the formation of phosphate films. However, at high temperatures, the dissolution degree of soluble phosphate ions increases, which results in some unwanted phosphate films (phosphate residues) deposited on the substrate, ultimately deteriorating the coating. Evidently, increasing the pH in a proper range at high temperatures eliminated phosphate residues and increased the deposition rate of phosphate films on the metal substrate. Cui *et al.* [61] reported that the optimal coating for Mn-PCC was formed at a temperature of 95°C and pH value between 3.5 and 4.5. The coating was uniform and compact, which consisted of $MnHPO_4{\cdot}2.25H_2O$ (12–15 μm), having the composition of O, Mg, P, Mn, and Al. The absence of toxic elements, such as Cr and F, rendered the film environment friendly. At high temperatures, fine grains of PCCs were formed, which resulted in high-density coatings. They found that for the Mn-PCC, E_{corr} was positively shifted by 102 mV, and i_{corr} was decreased by an order of four over the bare substrate. Furthermore, Li *et al.* [62] found that at high temperatures, alloys become corrosion resistant, and the highest E_{corr} was obtained at 90°C. However, a further increase in temperature resulted in the deposition of the phosphating product at the bottom of the beaker, thus reducing the coating deposition.

Li *et al.* [62] investigated the effect of pre-activation on the ZK60 alloy and found that samples with pre-activation exhibited fine and dense coatings, which reduced the porosity and increased the corrosion resistance. They reported that due to pre-activation, Mg phosphate was deposited on the substrate, which increased the nucleation density and produced fine grains. Moreover, pre-activation reduced the surface roughness, which was developed during polishing and facilitated the formation of PCCs with small grain sizes [23]. They reported that at a temperature of 90°C and immersion time of 20 min, a coating of manganese phosphate called hureaulite (33 μm) was formed, as shown in reaction (14).

$$5Mn^{2+} + 2(HPO_4)^{2-} + 2(PO_4)^{3-} + 4H_2O \rightarrow Mn_5(PO_4)_2(PO_3OH)_2 \cdot 4H_2O \downarrow \quad (14)$$

Zhang *et al.* [23] found that surface roughness affected coating deposition and observed that homogeneous and small-grain phosphate coating was obtained on surfaces with low roughness. On the surface with high roughness, a discontinuous coating was formed consisting of $MnHPO_4$ at the peak region and $MgHPO_4$ in the valley region, as shown in Fig. 8. The coating with high surface roughness was more prone to corrosion as compared to surfaces with low roughness. The details of the coating bath are found in Table 5 [25,58–63].

5.5. Other types

This section focuses on some of the other types of CCs, such as molybdate, permanganate, vanadium, and cerium-based phosphates. These types of coatings possess some advantages over coatings as discussed earlier. For instance, vanadium-based phosphate coatings exhibit self-healing properties, unlike Zn-PCC or Mg-PCC [64]. Moreover, studies have demonstrated that the corrosion resistance of permanganate and molybdate phosphate is comparable with that of chromate-based coatings [12,65].

Yong *et al.* [12] studied the comparison of molybdate/phosphate composite CC (Mo/P) and conventional molybdate (Mo). The coating of alveolate microstructure without cracks was formed in the molar ratio (1:2) of $MoO_4^{2-}/H_2PO_4^-$, which enhanced the corrosion performance. They reported that E_{corr} = −0.98 V and corrosion current ($\lg i_{corr}$ = −8.3 A) were higher than Mo. The presence of metaphosphate enhanced the deposition of conversion products having the composition of $Me_x(PO_4)_y$ (Me refers to metals such as Mn,

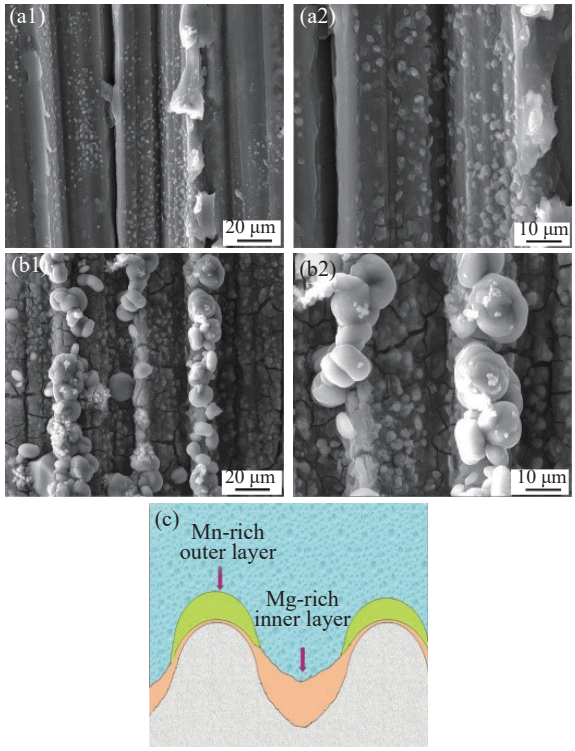

Fig. 8. SEM images of PCC (150 grit) in an Mn-PCC during coating formation process: (a1, a2) 10 s (a1 and a2 are with different magnifications) and (b1, b2) 180 s (b1 and b2 are with different magnifications); (c) schematic illustrating coating formation on the AZ91 alloy with a high surface roughness [23]. Reprinted from *Surf. Coat. Technol.*, 359, C.Y. Zhang, B. Liu, B.X. Yu, X.P. Lu, Y. Wei, T. Zhang, J.M.C. Mol, and F.H. Wang, Influence of surface pretreatment on phosphate conversion coating on AZ91 Mg alloy, 414-425, Copyright 2018, with permission from Elsevier.

Ca, and others), $MgAl_2O_4$, MgO, Al_2O_3, MnOOH, MnO, $CaMoO_4$, and MoO_3. However, an amorphous structure with cracks was observed for Mo coatings mainly consisting of $MgAl_2O_4$, MoO_3, MgO, Al_2O_3, and $CaMoO_4$.

Chong and Shih [65] developed a permanganate–phosphate coating on the AZ series and compared its performance with that of chromate-based coating. A layer of phosphate and metal oxide was formed after pickling with 75% (v/v) H_3PO_4 (v/v refers to volume by volume, a measure of volume concentration of a substance in solution), which reduced the galvanic effect. The coating consisted of oxides/hydroxides, such as MgO, $Mg(OH)_2$, $MgAl_2O_4$, Al_2O_3, $Al(OH)_3$, and MnO_2 or Mn_2O_3 having network-like cracks. The presence of $MgAl_2O_4$ and Al_2O_3 enhanced the corrosion resistance of the coating, making it comparable with conventional Cr^{6+} coating.

Zhao *et al.* [66] developed permanganate–phosphate CC to evaluate the effect of acid pickling. The coating with a uniform thickness of 7–10 μm was formed, which consisted of non-penetrable micropores of approximately 1 μm, thus enhancing the adhesion between coating and paints. pH (3.0–5.0) played a critical role in the compactness and adhesive ability of the coating. Salt spray tests (24 h, 5wt% NaCl) revealed that the average rusted area in the permanganate–phosphate coating was 12.72% lower than that in the chromate-based coating. However, Zucchi *et al.* [67] found that permanganate coatings consisted of layers with cracks, whereas stannate baths were composed of layers without any penetrating flaws, which resulted in higher initial corrosion resistance of stannate CCs.

Niu *et al.* [68] observed that in vanadate CC (VCC), the addition of vanadate ((NaVO$_3$, 4.0 g/L) promotes the film

Table 5. Bath composition and coating characteristics of the manganese phosphate conversion of coatings

Alloy	Bath composition	Process parameter			Coating characteristics & composition	Coating thickness / μm	E_{corr} / V	i_{corr} / (A·cm^{-2})	Ref.
		pH	Temp. / °C	Immersion time / min					
AZ91	$Mn(H_2PO_4)_2$: 20–50 g/L; H_3PO_4 (85wt%): 3–10 mL/L	2–3.5	45–75	10–30	Uniform, dense, and fine grain coating having composition of Mn, P, and O	n.d.	−0.139	n.d.	[58]
AZ31	$Mn(H_2PO_4)_2$: 40 g/L; polyphosphate: 0.54 g/L	3.5–4.5	95	25	Dense and fine grain; $MnHPO_4{\cdot}2.25H_2O$	12–15	−1.464	4.75×10^{-8}	[61]
AZ91D	$Mn(NO_3)_2$: 0.01 M; $NH_4H_2PO_4$: 0.01 M	4	80	5	Compact but thin and duplex layer coating; $Mg(OH)_2$ (inner layer) and$(Mg/Mn)_3(PO_4)_2$ (outer layer)	1.5	n.d.	n.d.	[63]
AZ31	$Mn(H_2PO_4)_2$: 35 g/L; Citric acid (additive): 0.5 g/L	2.5	95	20	Lamellar and block structure with no micro-crack exist with duplex layer coating; $MnHPO_4{\cdot}2.25H_2O$ (outer layer) and $Mg_3(PO_4)_2$, $AlPO_4$ (inner layer)	n.d.	−0.388	5×10^{-3}	[59]
AZ31	n.d.	3–6	95	25	Dense film free from other phosphate residues	n.d.	−1.496	1.368×10^{-7}	[60]
ZK60	$Mn(H_2PO_4)_2{\cdot}2H_2O$: 40 g/L; sodium citrate: 0.5 g/L; hexamethylenetetramine: 0.2 g/L	2.3	90	20	Compact with a fine crystal grain size of 15 μm; $Mn_5(PO_4)_2(PO_3OH)_2{\cdot}4H_2O$ (Hureaulite)	33	−0.85	2.94×10^{-9}	[62]
AZ91	NaH_2PO_4: 35 g/L; $(NH_4)_2HPO_4$: 5 g/L; $NaNO_3$: 2 g/L; $MnSO_4$: 35 g/L	3.5	60	10	Uniform and dense with duplex layer coating; $MgHPO_4$ (inner layer) and $MnHPO_4$ (outer layer)	n.d.	−1.445	4.8×10^{-6}	[23]

formation capability. SEM analysis revealed crack-free dense coatings with a fine crystalline structure having a good coating coverage area (coating deposition = 26.5 g/m^2), which comprised of vanadium, phosphorus, zinc, molybdenum, and oxygen. They observed that vanadate ions in the range of 4–5.5 g/L increased the adhesion between the electrophoretic paint coating and VCC due to the formation of the 3D net structure of the coating. Moreover, Zhou *et al.* [69] observed that calcium vanadium phosphate (P-Ca-V) coating exhibited the highest corrosion efficiency. They proposed a model for mitigating hydrogen-induced cracking in CCs and found that the dehydration effect plays a minor role during cracking phenomena. Sun *et al.* [50] reported that P-Ca-V coatings are mainly composed of $CaHPO_4$, $Ca_3(PO_4)_2$, and $Mg_3(PO_4)_2$. They studied the effects of vanadium concentration on the anti-corrosion property and found that P-Ca-V exhibited an enhanced corrosion resistance due to the self-healing property of vanadium.

Jian *et al.* [70] studied the effect of the addition of rare-earth metal cerium (Ce) on the corrosion performance of Mn-PCC on the LZ91 Mg alloy. For this study, two baths were prepared, i.e., Mn-Ce-P (with cerium) and Mn-P (without cerium). In Mn-Ce-P, the coating consisted of a duplex layer with a porous inner layer and compact outer layer, whereas relatively wider cracks were formed on Mn-P. With an optimum immersion time, the porous layer decreases, which leads to an increase in the thickness of the compact layer. They found that for an immersion time of 30 s, coatings with a thickness of 310 nm (Mn-Ce-P) and 810 nm (Mn-P) were formed on the substrate. Salt spray tests revealed that the corrosion area was reduced to 10% from 50% with the addition of Ce in the phosphate bath. Table 6 shows that for cerium-based phosphates, the immersion time and temperature are significantly low.

Jayaraj *et al.* [71] developed lanthanum-based phosphate coating on AZ31 Mg using a two-stage approach consisting of different solvents (water and ethanol) and studied their corrosion effectiveness. In the first stage, an Mg alloy was pretreated in an ammonium biphosphate solution ($NH_4H_2PO_4$), which resulted in the formation of struvite and newberyite phases. The second stage consisted of the treatment of a pretreated specimen in a lanthanum nitrate bath in water and ethanol as solvent. They found that the specimen treated with ethanol as a solvent and the predominant phase formed was $LaPO_4$ (La-P), whereas, in the case of water, $La(OH)_3$ was the primary phase. The corrosion resistance of the specimen prepared in ethanol as a solvent was higher than that of water. A compact, continuous, and uniform layer of La-P was formed in the ethanol bath, which had lesser cracks than $La(OH)_3$. It is primarily because the presence of hydroxide ions favored the crack formation during the drying stage, thus reducing the corrosion resistance.

The other types of PCCs seem to be promising, but they do have some issues. For example, phosphate–permanganate and molybdate-based coatings do not have the regenerative ability, unlike CCCs. Vanadium coatings are sensitive to alloy composition and are responsible for degrading the corrosion performance in certain Mg alloys, such as EL21 [72]. Cerium-based phosphate coatings are not cost-effective, and the scaling of such technologies is difficult.

6. Critical assessment of phosphate CCs

This section critically investigates some of the important aspects of PCCs on Mg alloys. The role of bath parameters, such as temperature, pH, immersion time, and additives, are explored for the design of CC baths. Moreover, the coatings consist of several surface defects, which might lead to the failure of components in real-life applications. The formation mechanism of these defects, along with some of the mitigation strategies, are also discussed here. Finally, the advantages and limitations of different techniques to evaluate the corrosion performance of coatings are elaborated.

6.1. Influence of process parameters and bath additives

In PCC, the process parameters (temperature, pH, and immersion time), bath additives, and compositional parameters play a vital role in coating formation. Usually, while designing a CC bath, one set of parameters is altered while keeping the others constant, and their influence on the corrosion behavior is analyzed to determine the optimum range. The effect of these parameters on PCCs has not yet been understood from a fundamental perspective. Phenomenologically, very high temperatures lead to the precipitation of phosphates in the solution bath and the formation of coatings with porosity and cracks [62]. Zeng *et al.* [73] studied the effect of bath temperatures (40–60°C) on the corrosion performance of a Zn–Ca-PCC on Mg–Li–Ca alloys. They observed that with the increase in temperature, the coatings obtained were dense, compact, and homogeneous. They found that the coated sample at 55°C exhibited the highest corrosion resistance, but with a further increase to 60°C, pores and cracks were observed on the coated surface. As phosphating is an endothermic reaction, the increase in temperature quickly facilitates a greater number of nucleation sites, thus leading to fine, dense, and uniform coatings. Typically, for a PCC, the reported temperature varies between 40 and 90°C in the absence of any rare-earth additives [59,62,73]. The presence of rare earth additives/accelerators facilitates coating formation at room temperature [70]. Some studies also indicate that high temperatures reduce the immersion time to a certain extent [34]. In the case of PCCs, the immersion time of the coating process usually varies between 10 and 20 min [35,74]. A very high immersion time might lead to the corrosion of the coated surface, thus diminishing the coating performance.

There must be an optimum balance of pH of the solution bath for the dissolution of Mg ions. If the pH is maintained too high, then the dissolution of Mg will be less, which may lead to a low deposition rate. Conversely, a low pH will result in the corrosion of the Mg substrate. Thus, an optimal pH must be maintained in the solution bath; otherwise, coating

Table 6. Bath composition and coating characteristics of the other types of phosphate CCs

Coating type	Alloy	Bath composition	Process parameter			Coating characteristics & composition	Coating thickness / μm	E_{corr} / V	i_{corr} / (A·cm^{-2})	Ref.
			pH	Temp. / °C	Immersion time / min					
Molybdate/ phosphate	AM60	Na_2MoO_4: 30 g/L; $Ca(NO_3)_2$: 4 g/L; $Mn(Ac)_2$: 6 g/L; additive: 1 g/L: $NaNO_3$: 1 g/L; NaH_2PO_4: 40 g/L	5	50	5	Homogeneous netlike coating/crack free with alveolate structure; $Me_x(PO_4)_y$, $MgAl_2O_4$, MgO, Al_2O_3, MnOOH, MnO, $CaMoO_4$, and MoO_3.	n.d.	−0.98	n.d.	[12]
Permanganate–phosphate	AZ61, AZ80, AZ91D	$KMnO_4$: 20 g/L; $MnHPO_4$: 60 g/L	n.d.	50	10	Having corrosion resistance equivalent to Cr^{6+} based coating; MgO, $Mg(OH)_2$, $MgAl_2O_3$, $Al(OH)_3$, MnO_2, and Mn_2O_3	3–5	−1.49, −1.5, −1.5	$10^{-4.01}$, $10^{-4.01}$, 10^{-4}	[65]
	AZ91D	$KMnO_4$: 40 g/L; K_2HPO_4: 150 g/L	3–5	40–70	10	Crystalline structure with light yellow to moderate orange having non-penetrating pores of less than 1 μm	7–10	−1.4529	5.858×10^{-4}	[66]
Vanadate–phosphate	AZ91D	Phosphoric acid: 10 g/L; $NaVO_3$: 4 g/L; zinc nitrate: 6.5–8.2 g/L; ammonium hydrogen fluoride: 1.0–1.6 g/L; ammonia solution: 1.5–6.5 mL/L; molybdate additive: 0.5–1.2 g/L	n.d.	50	10	Dense and refined crystalline structure and crack-free coating having excellent adhesion	n.d.	n.d.	n.d.	[68]
Manganese–cerium phosphate	LZ91	$KMnO_4$: 0.1 M; $Ce(NO_3)_3$: 0.02 M; $K_4P_2O_7$: 0.02 M	1.5	25	0.5	Dense and with self-healing coating; $MgHPO_4$, $Mg(PO_4)_2$, and $CePO_4$	0.31	−1.52	2.25×10^{-6}	[70]

defects, such as porosity, non-uniform coating growth, reduction in adhesiveness, and high surface roughness, are observed on the coated surface. Generally, the thermodynamic stability diagram is used to determine the requisite combination of metal ion concentration and pH for the precipitation of their respective insoluble metal phosphates. In the case of Zn-PCC, the reported pH range lies between 1.9 and 3.3 depending upon the Zn^{2+} concentration, whereas for Mg-PCC, the pH varies between 3 and 4.5 [35,54–55].

PCC baths for Mg alloys comprise a phosphate ion source (phosphoric acid or salt of any phosphate), metal salts (e.g., Ca^{2+}, Zn^{2+}, Mg^{2+}, and Mn^{2+}), and other additives such as oxidizing agents and inhibitors. The absence of metal salts in the coating bath yields the formation of Mg phosphates ($MgHPO_4$ or $Mg(PO_4)_2$) and hence failure to provide adequate corrosion protection. The addition of metal ions results in the precipitation of respective metal phosphates, which act as a protective outer layer. For instance, in the case of Zn-PCC, hopeite is precipitated on the specimen.

NO_3^- ions act as the oxidizing agent in a PCC bath. Their primary role is to oxidize Mg substrates and consume H^+ ions. Thus, they serve the dual purpose of increasing the dissolution rate of Mg and suppressing the H_2 evolution. Suppressed H_2 evolution is helpful in the formation of crack-free, compact, and dense coatings. Liao *et al.* [74] reported that 0.1 M of NO_3^- ions helped in the formation of compact and dense Mn-PCC. They found that excess NO_3^- ions (>0.75 M) produced a cracked inner layer of $MgHPO_4$ and inhibited coating deposition. This phenomenon can be attributed to the fact that excess NO_3^- ions can passivate the Mg surface, thus inhibiting the coating formation. Therefore, to achieve good results, the optimum concentration of NO_3^- ions must be used in the coating bath.

The addition of corrosion inhibitors in coating baths plays a critical role in protecting Mg substrates during the coating formation. When Mg is dipped into the solution bath of PCCs, Mg dissolves, and coating formation simultaneously takes place. However, after a certain coating time, if the dissolution rate is more than the coating formation rate, it might result in the corrosion of the substrate, thus leading to poor coating. Hence, the optimum concentration of corrosion inhibitors must be added to the bath.

6.2. Understanding the role of surface defects in PCCs

The presence of cracks, porosity, and non-uniform growth are some of the major surface defects of PCCs, which lead to localized corrosion. PCCs do not have self-healing properties, unlike chromate-based coatings, thus making them vulnerable to these defects. The primary reason for crack formation is the dehydration effect and entrapment of hydrogen atoms. During the drying stage, due to the evaporation of water molecules, the shrinkage of coating volume occurs, thus inducing cracks on coatings. Moreover, due to the cathodic reaction of the coating process, hydrogen atoms are produced on the surface and subsequently get adsorbed inside the coating, resulting in pore and crack formation. Typically,

cracks formed due to the dehydration effect occur at the outer layer with a wedge-like appearance [69]. On the contrary, cracks resulting from hydrogen entrapment are usually formed near the metal/coating interface [69]. Zhou *et al.* [69] proposed a model for hydrogen entrapped crack formation, the details of which are described in Fig. 9. They suggest that the sparse distribution of adsorbed hydrogen atoms will result in local defects. Conversely, the concentration of hydrogen atoms in a particular region might lead to the peeling of a large area, as shown in Fig. 9(h). Some strategies to mitigate the hydrogen-induced crack formation are the introduction of oxidizing agents, bath optimization for the promotion of codeposition of particles, and grain refinement. Strong oxidizing agents, such as VO_3^- (1 g/L), reduce the hydrogen entrapment at the metal/coating interface and improve the corrosion performance of the coating [69].

Usually, PCCs consist of two layers, where the inner layer consists of MgO, $MgHPO_4$, and compounds of other additives, whereas the outer layer comprises insoluble precipitates of respective metal phosphates. Typically, the Pilling–Bedworth (P–B) ratio between 1 and 2 is considered good for corrosion protection, whereas that below 1 results in poor protection [75]. Because the P–B ratio of MgO is ~0.8, it does not provide adequate protection against corrosion. However, the outer layer consisting of insoluble metal phosphates acts as a corrosion protective layer. The improper optimization of bath components sometimes leads to the formation of unwanted compounds, thus diminishing the compactness and favoring the crack formation and non-uniform growth. For example, the addition of excess fluoride salts favors the formation of MgF_2, which might hinder the dissolution of Mg and consequently lead to the formation of a non-uniform coating.

6.3. Critical assessment of corrosion evaluation techniques

Different techniques, such as PDP, EIS, immersion test, salt spray test, and hydrogen evolution measurement, are used for evaluating the corrosion performance of PCCs. These techniques have merits and limitations, and a single technique should not be used for evaluating the corrosion characteristic of PCCs.

Weight loss measurement is considered a benchmark test for evaluating the corrosion performance of coated specimens. Two types of weight loss measurement techniques, namely immersion and salt spray tests, are widely used. Usually, the weights of specimens before and after being exposed to a corrosive environment along with the exposure area are measured to estimate the corrosion rate. These tests indicate the average rate of corrosion taking place on the specimen over a period of time and are very sensitive to weight measurements. Weight measurements after being exposed to a corrosive environment is a critical step, and it is often difficult to remove corrosion products after the test, thus leading to improper estimation. Different cleaning procedures, such as dilute chromic acid (with silver and barium nitrate) and ul-

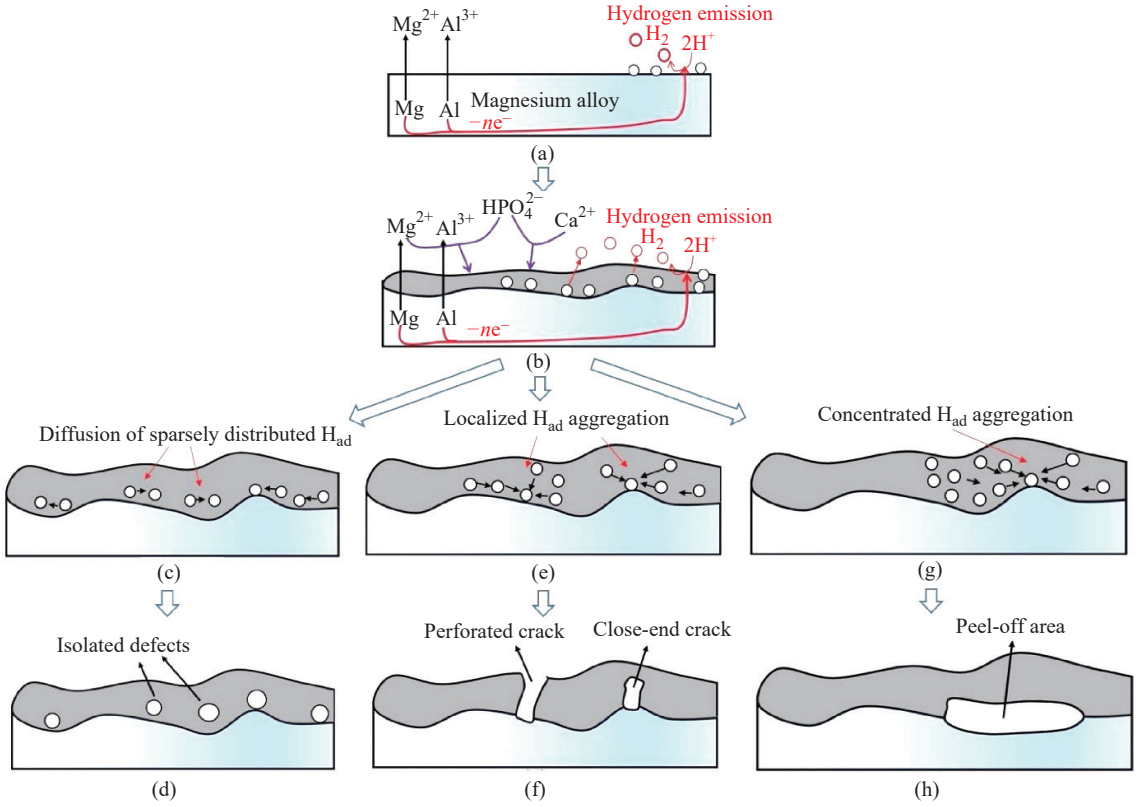

Fig. 9. Schematic of hydrogen-induced crack formation in phosphate conversion coatings [69]. Reprinted from *Surf. Corros. Sci.*, 178, P. Zhou, B.X. Yu, Y.J. Hou, G.Q. Duan, L.X. Yang, B. Zhang, T. Zhang, and F.H. Wang, Revisiting the cracking of chemical conversion coating on magnesium alloy, 109069, Copyright 2020, with permission from Elsevier.

trasonic cleaning with ethanol/acetone, are recommended for the removal of corrosion products from the substrate. Apart from measuring the corrosion rates, these methods are useful in analyzing the morphology of the exposed surface and understanding the corrosion mechanisms occurring on the specimen.

Electrochemical tests for estimating the corrosion rate of PCCs on Mg alloys, such as PDP and EIS, are widely popular. These tests provide an instantaneous corrosion rate and are simple to execute. Generally, to conduct electrochemical corrosion tests, a potentiostat is used with a three-electrode setup consisting of a working electrode (phosphate-coated specimen), reference electrode (Ag/AgCl or standard calomel electrode), and counter electrode (platinum). The main purpose of a counter electrode is to carry the current so that the potential difference between the working and reference electrodes is kept constant. Mg exhibits abnormal behaviors under anodic polarization due to the high hydrogen evolution, which is not in accordance with activation-controlled kinetics. This behavior of Mg is called the negative difference effect, the details of which can be found elsewhere [2,75]. The results obtained by extrapolating the Tafel slopes in a PDP experiment might not capture the true picture for phosphate-coated Mg alloys. Moreover, sometimes, PDP and weight loss measurements are not in agreement with each other for Mg alloys [2]. Hence, EIS is a relatively preferred electrochemical tool for Mg alloys instead of PDP.

Hydrogen collection is one of the classical methods used to measure the corrosion rate of PCC on Mg alloys. When the specimen is immersed in a corrosive environment (usually 3.5wt% NaCl), due to electrochemical reactions, Mg dissolves, and simultaneously H_2 evolves. Evidently, the evolution of 1 mol of H_2 gas is equivalent to the dissolution of 1 mol of Mg, and thus, the measurement of H_2 corresponds to the weight loss of the specimen. Moreover, H_2 evolution and weight loss are in agreement [2]. The volumetric approach for hydrogen collection is simple and widely adopted for evaluating the corrosion performance of phosphate-coated samples on Mg alloys. The basic setup for hydrogen collection consists of a beaker, burette, and funnel, as shown in Fig. 10. Some problems associated with the volumetric approach are sticking of hydrogen molecules at the walls of the funnel and insufficient volume of H_2 generation for corrosion resistance specimen, which lead to the underestimation of the corrosion rate.

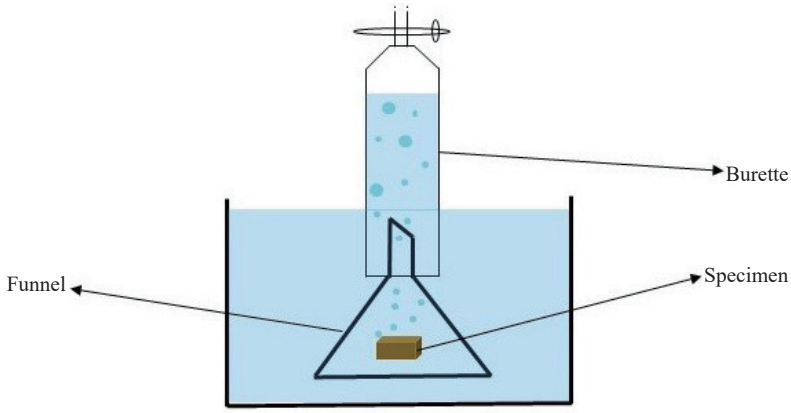

Fig. 10. Schematic overview of the hydrogen evolution measurement apparatus.

7. Conclusions and outlooks

The CC method is one of the widely used procedures to coat the underlying material for corrosion prevention. This review discusses different types of PCCs on Mg alloys, their mechanisms, and pretreatment techniques. The current developments of PCCs, advantages, limitations, and corrosion performance of coated samples are also discussed.

PCC is one of the most environment-friendly and cost-effective methods to coat underlying Mg substrates. The corrosion resistance of PCCs is comparable with that of chromate-based coatings due to the formation of a duplex layer structure. In fact, Zn-PCCs exhibit superior corrosion resistance in comparison to CCCs. The calcium-based phosphate coating on the Mg alloy produces HA, DCPD, and MWH, which are biocompatible, thus finding applications in human body implants and dentistry, among others. Vanadium-based coatings have self-healing properties, thus making them suitable as an additive in a coating bath. Results show that Mg-PCCs perform better in comparison to others under harsh conditions. One of the demerits of these coatings is the requirement for high temperatures and long immersion time. However, cerium-based phosphate coatings significantly lower the temperature and immersion time, thus improving the operational efficiency.

Some of the factors that play a crucial role in compact coating formation are bath composition, temperature, pH, thickness, porosities, cracks, and immersion time. In addition, the processing of Mg alloys plays a crucial role in increasing corrosion resistance. However, few studies have demonstrated the role of Mg processing techniques on corrosion. Recent advances in pretreatment technologies using laser emphasize that other advanced surface modification techniques, such as electron beam, plasma, and ion beam, should be further explored for superior performance.

Several chromium-free PCC technologies have been re-

ported in the literature, but the absence of large-scale usage of Mg in the automobile sector is concerning. Some of the major reasons for the lack of industrial usage are the presence of cracks, non-uniform growth of protective films on the underlying substrate, poor adhesion, and failure under harsh environments. The primary reason for the non-uniform coverage and crack formation is the dehydration effect and entrapped hydrogen gas inside the coating bath. A comprehensive and systematic understanding is primarily lacking due to the absence of standard protocols for benchmarking the corrosion performance investigation.

While the aqueous corrosion on the PCCs of Mg alloys is widely reported, the atmospheric corrosion has been largely neglected. Phosphate-coated samples lack self-healing properties, unlike chromate-based coatings. Therefore, the role of novel additives with self-repairing properties should be further investigated. In summary, new design principles, bath compositions, PCC mechanisms, and standard investigative tools must be formulated for developing advanced PCCs for different applications.

Acknowledgements

A. Kumar and K.K. Sahu acknowledge funding from Uchchatar Avishkar Yojna (UAY) (Phase II) project (code-IITBBS_004). D. Saran acknowledges funding from Prime Minister's Research Fellows (PMRF).

Conflict of Interest

The authors declare no potential conflict of interest.

References

[1] X.B. Chen, N. Birbilis, and T.B. Abbott, Review of corrosion-resistant conversion coatings for magnesium and its alloys, *Corrosion*, 67(2011), No. 3, art. No. 035005.

[2] G. Song, Recent progress in corrosion and protection of magnesium alloys, *Adv. Eng. Mater.*, 7(2005), No. 7, p. 563.

[3] J.E. Gray and B. Luan, Protective coatings on magnesium and its alloys—A critical review, *J. Alloys Compd.*, 336(2002), No. 1-2, p. 88.

[4] D.D. Zhang, F. Peng, and X.Y. Liu, Protection of magnesium alloys: From physical barrier coating to smart self-healing coating, *J. Alloys Compd.*, 853(2021), art. No. 157010.

[5] O. Gharbi, S. Thomas, C. Smith, and N. Birbilis, Chromate replacement: What does the future hold? *npj Mater. Degrad.*, 2(2018), art. No. 12.

[6] K.W. Cho, V.S. Rao, and H.S. Kwon, Microstructure and electrochemical characterization of trivalent chromium based conversion coating on zinc, *Electrochim. Acta*, 52(2007), No. 13, p. 4449.

[7] European Chemicals Agency (ECHA), *Understanding REACH*, 2007 [2021-12-31]. https://echa.europa.eu/regulations/reach/understanding-reach

[8] W.K. Chen, C.Y. Bai, C.M. Liu, C.S. Lin, and M.D. Ger, The effect of chromic sulfate concentration and immersion time on the structures and anticorrosive performance of the Cr(III) conversion coatings on aluminum alloys, *Appl. Surf. Sci.*, 256(2010), No. 16, p. 4924.

[9] S. Jana, M. Olszta, D. Edwards, M. Engelhard, A. Samanta, H.T. Ding, P. Murkute, O.B. Isgor, and A. Rohatgi, Microstructural basis for improved corrosion resistance of laser surface processed AZ31 Mg alloy, *Corros. Sci.*, 191(2021), art. No. 109707.

[10] M. Doerre, L. Hibbitts, G. Patrick, and N.K. Akafuah, Advances in automotive conversion coatings during pretreatment of the body structure: A review, *Coatings*, 8(2018), No. 11, art. No. 405.

[11] S. Pommiers, J. Frayret, A. Castetbon, and M. Potin-Gautier, Alternative conversion coatings to chromate for the protection of magnesium alloys, *Corros. Sci.*, 84(2014), p. 135.

[12] Z.Y. Yong, J. Zhu, C. Qiu, and Y.L. Liu, Molybdate/phosphate composite conversion coating on magnesium alloy surface for corrosion protection, *Appl. Surf. Sci.*, 255(2008), No. 5, p. 1672.

[13] V.S. Saji, Review of rare-earth-based conversion coatings for magnesium and its alloys, *J. Mater. Res. Technol.*, 8(2019), No. 5, p. 5012.

[14] S. Shadanbaz and G.J. Dias, Calcium phosphate coatings on magnesium alloys for biomedical applications: A review, *Acta Biomater.*, 8(2012), No. 1, p. 20.

[15] ASTM International, ASTM Standard B94-18: *Standard Specification for Magnesium-Alloy Die Castings*, ASTM International, West Conshohocken, PA, 2018.

[16] S.A. Salman, R. Ichino, and M. Okido, A comparative electrochemical study of AZ31 and AZ91 magnesium alloy, *Int. J. Corros.*, 2010(2010), art. No. 412129.

[17] H.Y. Yang, X.W. Guo, X.B. Chen, and N. Birbilis, A homogenisation pre-treatment for adherent and corrosion-resistant Ni electroplated coatings on Mg-alloy AZ91D, *Corros. Sci.*, 79(2014), p. 41.

[18] X.B. Chen, H.Y. Yang, T.B. Abbott, M.A. Easton, and N. Birbilis, Corrosion protection of magnesium and its alloys by metal phosphate conversion coatings, *Surf. Eng.*, 30(2014), No. 12, p. 871.

[19] L. Pezzato, D. Vranescu, M. Sinico, C. Gennari, A.G. Settimi, P. Pranovi, K. Brunelli, and M. Dabalà, Tribocorrosion properties of PEO coatings produced on AZ91 magnesium alloy with silicate- or phosphate-based electrolytes, *Coatings*, 8(2018), No. 6, art. No. 202.

[20] Z.M. Liu and W. Gao, Electroless nickel plating on AZ91 Mg alloy substrate, *Surf. Coat. Technol.*, 200(2006), No. 16-17, p. 5087.

[21] K. Brunelli, M. Dabalà, I. Calliari, and M. Magrini, Effect of HCl pre-treatment on corrosion resistance of cerium-based conversion coatings on magnesium and magnesium alloys, *Corros. Sci.*, 47(2005), No. 4, p. 989.

[22] W.J. Tomlinson and J.P. Mayor, Formation, microstructure, surface roughness, and porosity of electroless nickel coatings, *Surf. Eng.*, 4(1988), No. 3, p. 235.

[23] C.Y. Zhang, B. Liu, B.X. Yu, X.P. Lu, Y. Wei, T. Zhang, J.M.C. Mol, and F.H. Wang, Influence of surface pretreatment on phosphate conversion coating on AZ91 Mg alloy, *Surf. Coat. Technol.*, 359(2019), p. 414.

[24] T. Li, Z.J. Leng, S.F. Wang, X.T. Wang, R. Ghomashchi, Y.S. Yang, and J.X. Zhou, Comparison of the effects of pre-activators on morphology and corrosion resistance of phosphate conversion coating on magnesium alloy, *J. Magnes. Alloys*, (2021). DOI: 10.1016/j.jma.2021.03.012

[25] H.Y. Yang, X.B. Chen, X.W. Guo, G.H. Wu, W.J. Ding, and N. Birbilis, Coating pretreatment for Mg alloy AZ91D, *Appl. Surf. Sci.*, 258(2012), No. 14, p. 5472.

[26] Y.K. Zhang, J. You, J.Z. Lu, C.Y. Cui, Y.F. Jiang, and X.D. Ren, Effects of laser shock processing on stress corrosion cracking susceptibility of AZ31B magnesium alloy, *Surf. Coat. Technol.*, 204(2010), No. 24, p. 3947.

[27] J.Z. Lu, K.Y. Luo, Y.K. Zhang, C.Y. Cui, G.F. Sun, J.Z. Zhou,

L. Zhang, J. You, K.M. Chen, and J.W. Zhong, Grain refinement of LY2 aluminum alloy induced by ultra-high plastic strain during multiple laser shock processing impacts, *Acta Mater.*, 58(2010), No. 11, p. 3984.

[28] X.C. Zhang, F. Zhong, X.P. Li, B. Liu, C.Y. Zhang, B. Buhe, T. Zhang, G.Z. Meng, and F.H. Wang, The effect of hot extrusion on the microstructure and anti-corrosion performance of LDHs conversion coating on AZ91D magnesium alloy, *J. Alloys Compd.*, 788(2019), p. 756.

[29] G.Q. Hu, K. Guan, L.B. Lu, J.R. Zhang, N. Lu, and Y.C. Guan, Engineered functional surfaces by laser microprocessing for biomedical applications, *Engineering*, 4(2018), No. 6, p. 822.

[30] H.L. Liu, Z.P. Tong, Y. Yang, W.F. Zhou, J.N. Chen, X.Y. Pan, and X.D. Ren, Preparation of phosphate conversion coating on laser surface textured surface to improve corrosion performance of magnesium alloy, *J. Alloys Compd.*, 865(2021), art. No. 158701.

[31] H.L. Liu, Z.P. Tong, W.F. Zhou, Y. Yang, J.F. Jiao, and X.D. Ren, Improving electrochemical corrosion properties of AZ31 magnesium alloy *via* phosphate conversion with laser shock peening pretreatment, *J. Alloys Compd.*, 846(2020), art. No. 155837.

[32] M.A. Hafeez, A. Farooq, A. Zang, A. Saleem, and K.M. Deen, Phosphate chemical conversion coatings for magnesium alloys: A review, *J. Coat. Technol. Res.*, 17(2020), No. 4, p. 827.

[33] A. Pragatheeswaran, P.V. Ananthapadmanabhan, Y. Chakravarthy, S. Bhandari, V. Chaturvedi, A. Nagaraj, and K. Ramachandran, Plasma spray-deposited lanthanum phosphate coatings for protection against molten uranium corrosion, *Surf. Coat. Technol.*, 265(2015), p. 166.

[34] Y.L. Cheng, H.L. Wu, Z.H. Chen, H.M. Wang, and L.L. Li, Phosphating process of AZ31 magnesium alloy and corrosion resistance of coatings, *Trans. Nonferrous Met. Soc. China*, 16(2006), No. 5, p. 1086.

[35] R. Amini and A.A. Sarabi, The corrosion properties of phosphate coating on AZ31 magnesium alloy: The effect of sodium dodecyl sulfate (SDS) as an eco-friendly accelerating agent, *Appl. Surf. Sci.*, 257(2011), No. 16, p. 7134.

[36] L.Y. Niu, J.X. Lin, Y. Li, Z.M. Shi, and L.C. Xu, Improvement of anticorrosion and adhesion to magnesium alloy by phosphate coating formed at room temperature, *Trans. Nonferrous Met. Soc. China*, 20(2010), No. 7, p. 1356.

[37] Q. Li, S.Q. Xu, J.Y. Hu, S.Y. Zhang, X.K. Zhong, and X.K. Yang, The effects to the structure and electrochemical behavior of zinc phosphate conversion coatings with ethanolamine on magnesium alloy AZ91D, *Electrochim. Acta*, 55(2010), No. 3, p. 887.

[38] N.V. Phuong, K.H. Lee, D. Chang, and S. Moon, Effects of Zn^{2+} concentration and pH on the zinc phosphate conversion coatings on AZ31 magnesium alloy, *Corros. Sci.*, 74(2013), p. 314.

[39] W. Shang, C.B. He, Y.Q. Wen, Y.Y. Wang, and Z. Zhang, Performance evaluation of triethanolamine as corrosion inhibitor for magnesium alloy in 3.5 wt% NaCl solution, *RSC Adv.*, 6(2016), No. 115, p. 113967.

[40] S.C.G. Leeuwenburgh, M.C. Heine, J.G.C. Wolke, S.E. Pratsinis, J. Schoonman, and J.A. Jansen, Morphology of calcium phosphate coatings for biomedical applications deposited using Electrostatic Spray Deposition, *Thin Solid Films*, 503(2006), No. 1-2, p. 69.

[41] Y.C. Su, Y.T. Guo, Z.L. Huang, Z.H. Zhang, G.Y. Li, J.S. Lian, and L.Q. Ren, Preparation and corrosion behaviors of calcium phosphate conversion coating on magnesium alloy, *Surf. Coat. Technol.*, 307(2016), p. 99.

[42] B. Liu, X. Zhang, G.Y. Xiao, and Y.P. Lu, Phosphate chemical conversion coatings on metallic substrates for biomedical application: A review, *Mater. Sci. Eng. C*, 47(2015), p. 97.

[43] Y.C. Su, Y.C. Su, Y.B. Lu, J.S. Lian, and G.Y. Li, Composite microstructure and formation mechanism of calcium phosphate conversion coating on magnesium alloy, *J. Electrochem. Soc.*, 163(2016), No. 9, p. G138.

[44] P. Amaravathy and T.S. Sampath Kumar, Novel strontium doped zinc calcium phosphate conversion coating on AZ31 magnesium alloy for biomedical applications, *J. Biomimetics Biomater. Biomed. Eng.*, 34(2017), p. 57.

[45] W. Zai, X.R. Zhang, Y.C. Su, H.C. Man, G.Y. Li, and J.S. Lian, Comparison of corrosion resistance and biocompatibility of magnesium phosphate (MgP), zinc phosphate (ZnP) and calcium phosphate (CaP) conversion coatings on Mg alloy, *Surf. Coat. Technol.*, 397(2020), art. No. 125919.

[46] Y.T. Guo, Y.C. Su, R. Gu, Z.H. Zhang, G.Y. Li, J.S. Lian, and L.Q. Ren, Enhanced corrosion resistance and biocompatibility of biodegradable magnesium alloy modified by calcium phosphate/collagen coating, *Surf. Coat. Technol.*, 401(2020), art. No. 126318.

[47] D. Liu, Y.Y. Li, Y. Zhou, and Y.G. Ding, The preparation, characterization and formation mechanism of a calcium phosphate conversion coating on magnesium alloy AZ91D, *Materials (Basel)*, 11(2018), No. 6, art. No. 908.

[48] X.B. Chen, N. Birbilis, and T.B. Abbott, Effect of $[Ca^{2+}]$ and $\left[PO_4^{3-}\right]$ levels on the formation of calcium phosphate conversion coatings on die-cast magnesium alloy AZ91D, *Corros. Sci.*, 55(2012), p. 226.

[49] R.C. Zeng, Z.D. Lan, L.H. Kong, Y.D. Huang, and H.Z. Cui, Characterization of calcium-modified zinc phosphate conversion coatings and their influences on corrosion resistance of AZ31 alloy, *Surf. Coat. Technol.*, 205(2011), No. 11, p. 3347.

[50] R.X. Sun, S.K. Yang, and T. Lv, Corrosion behavior of AZ91D magnesium alloy with a calcium–phosphate–vanadium composite conversion coating, *Coatings*, 9(2019), No. 6, art. No. 379.

[51] M.F. Morks, Magnesium phosphate treatment for steel, *Mater. Lett.*, 58(2004), No. 26, p. 3316.

[52] N. van Phuong and S. Moon, Comparative corrosion study of zinc phosphate and magnesium phosphate conversion coatings on AZ31 Mg alloy, *Mater. Lett.*, 122(2014), p. 341.

[53] M. Fouladi and A. Amadeh, Comparative study between novel magnesium phosphate and traditional zinc phosphate coatings, *Mater. Lett.*, 98(2013), p. 1.

[54] W. Zai, Y.C. Su, H.C. Man, J.S. Lian, and G.Y. Li, Effect of pH value and preparation temperature on the formation of magnesium phosphate conversion coatings on AZ31 magnesium alloy, *Appl. Surf. Sci.*, 492(2019), p. 314.

[55] J. Jayaraj, S. Amruth Raj, A. Srinivasan, S. Ananthakumar, U.T.S. Pillai, N.G.K. Dhaipule, and U.K. Mudali, Composite magnesium phosphate coatings for improved corrosion resistance of magnesium AZ31 alloy, *Corros. Sci.*, 113(2016), p. 104.

[56] N. van PHUONG, M. Gupta, and S. Moon, Enhanced corrosion performance of magnesium phosphate conversion coating on AZ31 magnesium alloy, *Trans. Nonferrous Met. Soc. China*, 27(2017), No. 5, p. 1087.

[57] W.Q. Zhou, D.Y. Shan, E.H. Han, and W. Ke, Structure and formation mechanism of phosphate conversion coating on die-cast AZ91D magnesium alloy, *Corros. Sci.*, 50(2008), No. 2, p. 329.

[58] W.Q. Zhou, W. Tang, Q. Zhao, S.W. Wu, and E.H. Han, Influence of additive on structure and corrosion resistance of manganese phosphate film on AZ91 magnesium alloy, *Mater. Sci. Forum*, 686(2011), p. 176.

[59] X.J. Cui, C.H. Liu, R.S. Yang, Q.S. Fu, X.Z. Lin, and M. Gong, Duplex-layered manganese phosphate conversion coating on AZ31 Mg alloy and its initial formation mechanism, *Corros. Sci.*, 76(2013), p. 474.

[60] X.J. Cui, C.H. Liu, R.S. Yang, X.Z. Lin, and M. Gong, Prepara-

tion and characterization of phosphate film for magnesium alloy AZ31, *Phys. Procedia*, 25(2012), p. 194.
[61] X.J. Cui, C.H. Liu, R.S. Yang, M.T. Li, X.Z. Lin, and M. Gong, Phosphate film free of chromate, fluoride and nitrite on AZ31 magnesium alloy and its corrosion resistance, *Trans. Nonferrous Met. Soc. China*, 22(2012), No. 11, p. 2713.
[62] T. Li, S.F. Wang, H.T. Liu, J.H. Wu, S.Q. Tang, Y.S. Yang, X.T. Wang, and J.X. Zhou, Improved corrosion resistance of Mg alloy by a green phosphating: Insights into pre-activation, temperature, and growth mechanism, *J. Mater. Sci.*, 56(2021), No. 1, p. 828.
[63] X.B. Chen, X. Zhou, T.B. Abbott, M.A. Easton, and N. Birbilis, Double-layered manganese phosphate conversion coating on magnesium alloy AZ91D: Insights into coating formation, growth and corrosion resistance, *Surf. Coat. Technol.*, 217(2013), p. 147.
[64] A.S. Hamdy, I. Doench, and H. Möhwald, Assessment of a one-step intelligent self-healing vanadia protective coatings for magnesium alloys in corrosive media, *Electrochim. Acta*, 56(2011), No. 5, p. 2493.
[65] K.Z. Chong and T.S. Shih, Conversion-coating treatment for magnesium alloys by a permanganate–phosphate solution, *Mater. Chem. Phys.*, 80(2003), No. 1, p. 191.
[66] M. Zhao, S.S. Wu, J.R. Luo, Y. Fukuda, and H. Nakae, A chromium-free conversion coating of magnesium alloy by a phosphate-permanganate solution, *Surf. Coat. Technol.*, 200(2006), No. 18-19, p. 5407.
[67] F. Zucchi, A. Frignani, V. Grassi, G. Trabanelli, and C. Monticelli, Stannate and permanganate conversion coatings on AZ31 magnesium alloy, *Corros. Sci.*, 49(2007), No. 12, p. 4542.
[68] L.Y. Niu, S.H. Chang, X. Tong, G.Y. Li, and Z.M. Shi, Analysis of characteristics of vanadate conversion coating on the surface of magnesium alloy, *J. Alloys Compd.*, 617(2014), p. 214.
[69] P. Zhou, B.X. Yu, Y.J. Hou, G.Q. Duan, L.X. Yang, B. Zhang, T. Zhang, and F.H. Wang, Revisiting the cracking of chemical conversion coating on magnesium alloys, *Corros. Sci.*, 178(2021), art. No. 109069.
[70] S.Y. Jian, Y.C. Tzeng, M.D. Ger, K.L. Chang, G.N. Shi, W.H. Huang, C.Y. Chen, and C.C. Wu, The study of corrosion behavior of manganese-based conversion coating on LZ91 magnesium alloy: Effect of addition of pyrophosphate and cerium, *Mater. Des.*, 192(2020), art. No. 108707.
[71] J. Jayaraj, K.R. Rajesh, S. Amruth Raj, A. Srinivasan, S. Ananthakumar, N.G.K. Dhaipule, S.K. Kalpathy, U.T.S. Pillai, and U.K. Mudali, Investigation on the corrosion behavior of lanthanum phosphate coatings on AZ31 Mg alloy obtained through chemical conversion technique, *J. Alloys Compd.*, 784(2019), p. 1162.
[72] H.A. Salam, I. Doench, and H. Moehwald, The effect of vanadia surface treatment on the corrosion inhibition characteristics of an advanced magnesium elektron 21 alloy in chloride media, *Int. J. Electrochem. Sci.*, 7(2012), No. 9, p. 7751.
[73] R.C. Zeng, X.X. Sun, Y.W. Song, F. Zhang, S.Q. Li, H.Z. Cui, and E.H. Han, Influence of solution temperature on corrosion resistance of Zn–Ca phosphate conversion coating on biomedical Mg–Li–Ca alloys, *Trans. Nonferrous Met. Soc. China*, 23(2013), No. 11, p. 3293.
[74] S.J. Liao, B.X. Yu, X.L. Zhang, X.P. Lu, P. Zhou, C.Y. Zhang, X.B. Chen, T. Zhang, and F.H. Wang, New design principles for the bath towards chromate- and crack-free conversion coatings on magnesium alloys, *J. Magnes. Alloys*, 9(2021), No. 2, p. 505.
[75] M. Esmaily, J.E. Svensson, S. Fajardo, N. Birbilis, G.S. Frankel, S. Virtanen, R. Arrabal, S. Thomas, and L.G. Johansson, Fundamentals and advances in magnesium alloy corrosion, *Prog. Mater. Sci.*, 89(2017), p. 92.